https://ntrs.nasa.gov/search.jsp?R=19790008383 2020-03-22T01:40:51+00:00Z

General Disclaimer

One or more of the Following Statements may affect this Document

- This document has been reproduced from the best copy furnished by the organizational source. It is being released in the interest of making available as much information as possible.

- This document may contain data, which exceeds the sheet parameters. It was furnished in this condition by the organizational source and is the best copy available.

- This document may contain tone-on-tone or color graphs, charts and/or pictures, which have been reproduced in black and white.

- This document is paginated as submitted by the original source.

- Portions of this document are not fully legible due to the historical nature of some of the material. However, it is the best reproduction available from the original submission.

Produced by the NASA Center for Aerospace Information (CASI)

CR 151881

SIMPLE MODELS FOR THE SHUTTLE REMOTE MANIPULATOR SYSTEM

W. T. Fowler
B. D. Tapley
B. E. Schutz

(NASA-CR-151881) SIMPLE MODELS FOR THE SHUTTLE REMOTE MANIPULATOR SYSTEM Final Report (Texas Center for Research) 63 p HC A04/MF A01 CSCL 05H

N79-16554

Unclas
G3/54 43559

Texas Center for Research
3100 Perry Lane
Austin, Texas

This document is the final report under Contract NAS 9-15385.

TABLE OF CONTENTS

SIMPLE MODELS FOR THE SHUTTLE REMOTE MANIPULATOR SYSTEM

Introduction

One of the fundamental objectives of the NASA Space Shuttle Mission is to develop the capability to launch and retrieve payloads from near-earth orbit using the reusable shuttle orbiter vehicle. One of the more demanding of the early space shuttle missions will be the deployment of the Interium Upper Stage (IUS) which is currently under development for the Department of Defense. The primary function of the IUS will be to place a single large spacecraft or multiple smaller spacecraft in earth orbits which differ from the shuttle orbit or to place planetary spacecraft on earth-escape trajectories. The IUS-vehicle will be approximately sixty feet long and cylindrical in shape with a diameter of about fourteen feet. The overall weight of the IUS can be as much as 60,000 lb, which will be about one third of the overall shuttle-orbiter weight. The IUS will rely on a three-axis stabilized propulsion and avionic system for trajectory and attitude control. As a consequence, it is critical that the IUS spacecraft module be deployed in a stable attitude for check-out and launch. In the event of malfunction during the deployment stage, it will be necessary that the IUS module be recovered and returned to the shuttle payload bay. Hence, the RMS must be able to accomodate each of these operations.

The requirement that these manuevers be conducted while the shuttle and IUS are in close proximity without disturbing the attitude of the IUS vehicle, lead to several critical operational requirements. One of the primary problems associated with this close proximity operation arises from the IUS interactions with the shuttle RCS thruster plume. Any translational motion required by the shuttle for station-keeping and/or

rendezvous purposes must be performed using the 900 lb RCS thrusters. Since the projected area of the 60 feet long by 14 foot diameter IUS module will be on the order of 840 square feet, a substantial force can be generated by the pressure of the RCS jet plume. Since, in general, the center of pressure will not coincide with the center of mass, this interaction will lead to significant moments on the IUS. Tumbling and/or severe disturbances in the IUS attitude may occur. If these moments are introduced during the retrieve stage, severe forces and moments may be introduced in the remote manipulation system RMS/arm. Such moments may lead to structural failure of the RMS arm.

In addition, a careful study of the effects of the shuttle RCS thruster actuation during any of the close proximity maneuvers must be made. The primary questions of concern are those related to the effects of the moments on the IUS module. the forces generated on the RMS arm, control strategies and limitations on the RMS arm movement to prevent damage and, finally, thruster firing limitations to prevent unacceptable moments on the IUS.

The basic RMS design calls for two manipulator arms and the supporting equipment for the operation of the arms. One manipulator arm will be mounted on the port side of the payload bay on all missions. The second arm will be installed on the starboard side of the payload bay and will be removable, if it is not required during a given mission. The RMS will be composed of the following major components: (a) two manipulator arms, (b) the RMS displays and control, and (c) the manipulator control interface unit. These components will be supported by the associated RMS software as well as the RMS ground control equipment. As with all space rated systems, weight and power requirement must be kept to a minimum. This leads to severe design

requirements which can be met if all pertinent factors are included in the design process.

While the state-of-art in the design and utilization of fixed-based remote manipulator systems has achieved a comparatively high degree of sophistication through medical and industrial applications, the specific applications of this technology to the shuttle remote manipulator system is not a direct extension of the current practice. The fundamental difference between the shuttle problem and those previously treated lies in the fact that the shuttle will be operating in an orbiting environment. As a consequence, the shuttle and the associated payload, which is either to be deployed or retrieved, will be interacting in an essentially zero-gravity environment. In this situation, unbalanced forces developed due to the mutual shuttle-payload interactions will cause rotational motions about the center of mass of both the shuttle and the payload. Since the RMS arm will be required either to move to accomodate these relative motions or to counter the motion by elastic deformation, severe design restraints are placed on the operation and control of both the shuttle and the RMS in the payload deployment/retrieval mode. Pre-launch study of the IUS operation can be accomplished only through numerically simulated studies. The simulation models will be complex since a number of factors will contribute to the phenomena under study. However, the models and the associated computer simulation program will serve as basic mission analysis tools. Consequently, it is mandatory that NASA develop a comprehensive understanding of the characteristics, accuracy, and limitations of the computer program simulations.

Computer programs which give reasonable complete descriptions of the motion are described in Refs. 2 and 3. The computing effort required to simulate motions of the arm with these models is quite severe and hence

case studies cannot be made in real time. In addition, there is significant computation costs associated with exercising computer programs based on complete mathematical models. As a consequence, simple models which contain the essential characteristics of the dynamic motion are of interest for pre-mission design studies. The models would be useful for performing a number of case studies rapidly with minimal computer costs. The conclusions reached after study with such models would then lead to a limited number of special cases which would be studied in detail by the more precise mathematical models. With this objective in mind, this investigation is aimed at establishing a series of simple models which can be used to study the forces and moments which occur due to the RCS jet plume firings during a deployment or retrieval of an IUS type payload. The models considered in this investigation are primarily planar in nature. The extension to three-dimensional motion is straightforward and will be addressed in subsequent studies. In this study primary attention is given to the roles the payload play in determining the overall moments on the arm.

Approach

In order to gain insight into the overall dynamics, the planar model of the space shuttle/RMS/payload system shown in Fig. 1.1 is considered. As stated previously, the primary objective of the analysis will be to characterize the forces and moments at the shoulder of the RMS (point a) as a function of the thruster force, $\overline{T}$. The analysis will be developed in several stages. In the first stage, the shuttle/RMS/payload combination will be assumed to be totally rigid. After considering the equations of motion for this model, a model with a linear spring at the shoulder, a, will be developed. The model will then be extended to include linear springs at both a and b. In each analysis, force and loading moments at a will be identified. Following a complete study of the single joint model, similar studies will be made of a two-joint model in which the arm is separated into two segments connected by linear spring at the midpoint C.

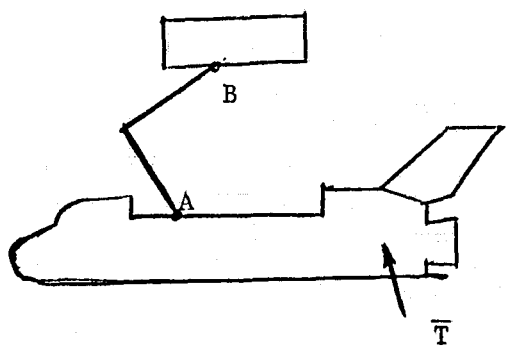

Figure I.1: Shuttle/RMS/Payload Model

The analysis will be developed in several steps. In the first step, the Shuttle/RMS/Payload combination will be assumed to be totally rigid. Next, a model with a linear spring at A will be developed. Then a model with linear springs at A and B will be considered. In each analysis, forces and bending moments at A will be sought.

I. RIGID BODY MODEL

In this model, the shuttle, arm, and payload are assumed to be a single rigid body. The geometry is shown below in Figure I.2.

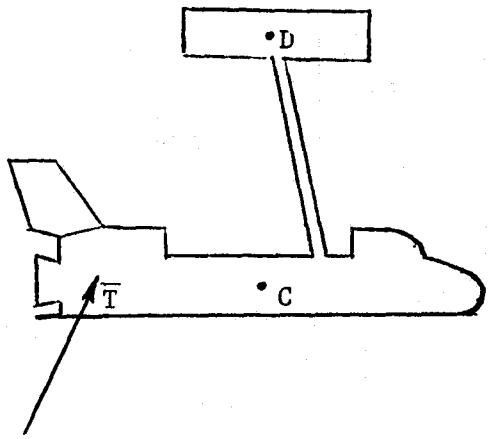

Figure I.2: Rigid Body Model

The point C is the center of mass of the shuttle, the point D is the center of mass of the payload, and the thruster applies a thrust $\bar{T}$ and a torque $\bar{M}_T$ about the shuttle center of mass.

The equations of motion for the system can be written in terms of the overall system center of mass G defined by

$$\bar{r}_G = \frac{\bar{r}_c m_s + \bar{r}_p m_p}{m_s + m_p} \qquad (I.1)$$

or, in terms of the motion of the center of mass, C, of the shuttle. Analyses based on G and C will be presented for comparison and to lay the groundwork for the more complex models to follow.

Motion Referenced to System c.m.,G:

The free-body diagram for the system is shown in Figure I.3.

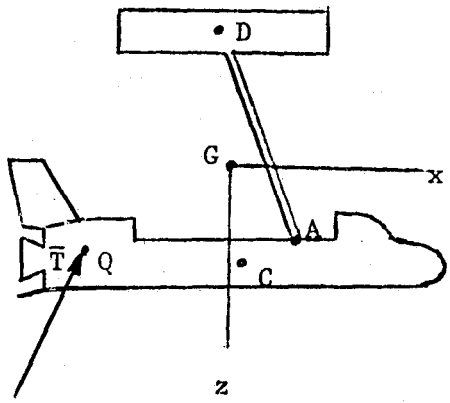

Figure I.3: Rigid Body Model Coordinates

The overall goal of the analysis is, as stated earlier, to derive forces and bending moments at the shoulder, point A. The pertinent equations are:

$$\Sigma F_x = T_x = (m_s + m_p)\, a_{G_x}$$

$$\Sigma F_z = T_z = (m_s + m_p)\, a_{G_z} \qquad \text{(I.2)}$$

$$\Sigma M_G = \bar{r}_{GQ} \times \bar{T} = I_G\, \alpha$$

Since the selection of a thruster gives the components of $\bar{T}$, and the specified shuttle-payload geometry gives $\bar{r}_{GQ}$, equations (I.2) form three equations in the three unknowns a_{G_x}, a_{G_z}, and α.

The geometry needed to determine $\bar{r}_{GQ}$ is simple since $\bar{r}_G$, $\bar{r}_C$, and $\bar{r}_{CQ}$ are known

$$\bar{r}_Q = \bar{r}_C + \bar{r}_{CQ}$$
$$\bar{r}_{GQ} = \bar{r}_Q - \bar{r}_G \qquad \text{(I.3)}$$

To find the forces and bending moments at A induced by the thruster firing, a free body diagram of the shuttle alone is necessary (see Figure I.4).

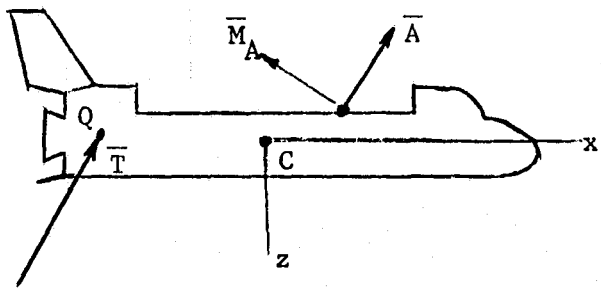

Figure I.4: Shuttle Free Body Diagram

For the shuttle,

$$\Sigma F_x = A_x + T_x = m_s a_{c_x}$$
$$\Sigma F_z = A_z + T_z = m_s a_{c_z} \qquad \text{(I.4)}$$
$$\Sigma M_C = M_A + \bar{r}_{CA} \times \bar{A} + r_{CQ} \times \bar{T} = I_{yy_s} \alpha$$

The unknowns are A_x, A_z, M_A, a_{C_x}, and a_{C_z}. From kinematics, the acceleration of C is related to the acceleration of G by

$$\bar{a}_c = \bar{a}_G + \bar{\omega} \times (\bar{\omega} \times \bar{r}_{GC}) + \bar{\alpha} \times \bar{r}_{GC} \qquad \text{(I.5)}$$

For the two-dimensional model, this vector equation results in two scalar equations. One new unknown is introduced, ω. However, ω is related to α by $\alpha = d\omega/dt$. Thus, a value is needed only for ω_o.

In scalar form, the equations necessary for this analysis are as follows. Let the origin of the chosen coordinate system be located at the initial location of the system center of mass and be translating along with it. When a thruster is fired, of course, the center of mass, G, will move away from the origin of the coordinates. Thus,

$$\bar{r}_{G_o} = 0\bar{i} + 0\bar{k}$$
$$\bar{V}_{G_o} = 0\bar{i} + 0\bar{k} \qquad \text{(I.6)}$$

The analysis is much simplified if the thrust firing is represented by an impulsive change. Equations (I.2) become, considering equations (I.6)

$$V_{G_x} = \frac{1}{(m_s + m_p)} \left(\int T_x dt\right)$$
$$V_{G_z} = \frac{1}{(m_s + m_p)} \left(\int T_z dt\right) \qquad \text{(I.7)}$$
$$\omega = \omega_o + \frac{1}{I_G} \left[\bar{r}_{GQ} \times \int \bar{T} dt\right]$$

In the third of equations (I.7),

$$\bar{r}_{GQ} = \bar{r}_Q - \bar{r}_G$$

but initially $\bar{r}_G \equiv 0$. Also

$$\bar{r}_Q = \bar{r}_C + \bar{r}_{CQ}$$
$$\bar{r}_Q = (x_C + x_{CQ})\bar{i} + (z_C + z_{CQ})\bar{k}$$
$$= x_Q\bar{i} + z_Q\bar{k}$$

Also

$$\bar{T} = T_x\bar{i} + T_z\bar{k}$$

and

$$\bar{r}_{GQ} \times \bar{T} = (z_Q T_x - x_Q T_z)\bar{j} \qquad \text{(I.8)}$$

Thus, if a constant thrust over a time of 0.1 is assumed, equations (I.7) become

$$V_{G_x} = \frac{0.1T_x}{(m_s + m_p)}$$
$$V_{G_z} = \frac{0.1T_z}{(m_s + m_p)} \qquad \text{(I.9)}$$
$$\omega = \omega_o + \frac{z_Q T_x - x_Q T_z}{10\ I_G}$$

Equations (I.9) determine the velocity of the system center of mass and the angular velocity at the end of any given impulsive firing of the thrusters. This information will be used to determine steady-state loads. For dynamic loads, as the thruster is fired it is necessary to return to Equations (I.2).

Equations (I.2) can be rewritten as

$$a_{G_x} = \frac{T_x}{(m_p + m_s)}$$
$$a_{G_z} = \frac{T_z}{(m_p + m_s)} \qquad \text{(I.10)}$$
$$\alpha = \frac{z_Q T_x - x_Q T_z}{I_G}$$

These three equations give a_{G_x}, a_{G_z} and α explicitly. Considering ω as a known parameter for the analysis which can be varied to determine its effects, the acceleration of the shuttle center of mass, C, can be formed using equation (I.5). For this purpose, let

$$\bar{r}_{GC} = x_{GC}\,\bar{i} + z_{GC}\,\bar{k}$$
$$\bar{\omega} = \omega\bar{j}$$
$$\bar{\alpha} = \alpha\bar{j}$$

Thus, from equation (I.5)

$$a_{C_x} = a_{G_x} - \omega^2 x_{GC} + z_{GC}\,\alpha$$
$$a_{C_z} = a_{G_z} - \omega^2 z_{GC} - x_{GC}\,\alpha \qquad \text{(I.11)}$$

Equations (I.11) give a_{C_x} and a_{C_z} explicitly in terms of known quantities. Next, A_x and A_z can be determined from equations (I.4) as

$$A_x = m_s a_{C_x} - T_x$$
$$A_z = m_s a_{C_z} - T_z \qquad \text{(I.12)}$$

Finally, M_A can be determined from the third of equations (I.4) as

$$M_A = I_{YYS} - z_{CQ}T_x + x_{CQ}T_z - z_{CA}A_x + x_{CA}A_z \qquad \text{(I.13)}$$

Equations (I.10), (I.11), (I.12), and (I.13) form the computation sequence for A_x, A_z and M_A in the rigid body case for any thruster. The parameters which must be specified are:

Choice of Thruster:	$(T_x, T_z, x_{CQ}, z_{CQ})$
Payload Location and Mass:	(m_p, x_C, z_C, I_{yyp})
Shuttle Parameters:	(I_{yys}, m_s)
Overall System Parameters:	I_G is given by geometry, I_{yys}, and I_{yyp}

II. SINGLE JOINT MODEL

The forces and torques acting on the shuttle are as shown below in Figure II.1.

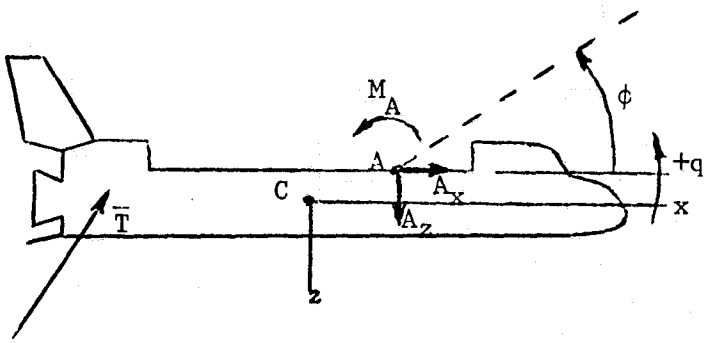

Figure II.1: Shuttle Free Body Diagram

$$\bar{T} = T_x\bar{i} + \cancel{T_y\bar{j}}^{\,0} + T_z\bar{k}$$

$$\bar{A} = A_x\bar{i} + \cancel{A_y\bar{j}}^{\,0} + A_z\bar{k}$$

$$\bar{V}_C = u\,\bar{i} + \cancel{v\,\bar{j}}^{\,0} + w\,\bar{k}$$

$$\bar{r}_{CA} = x_{CA}\bar{i} + \cancel{y_{CA}\bar{j}}^{\,0} + z_{CA}\bar{k}$$

$$\bar{M}_A = \cancel{L_A\bar{i}}^{\,0} + M_A\bar{j} + \cancel{N_A\bar{k}}^{\,0}$$

$$\bar{M}_T = \cancel{L_T\bar{i}}^{\,0} + M_T\bar{j} + \cancel{N_T\bar{k}}^{\,0}$$

where the quantities marked through are zero because of the assumption of planar motion. The xyz coordinate system is centered at the shuttle center of mass, C,

and rotates with the shuttle. The force $\bar{A}$ is the force exerted by the RMS on the shuttle at the shoulder and the force $\bar{T}$ is the force exerted on the shuttle by the firing of a thruster. In the current model, any thruster can be selected to exert the force $\bar{T}$. The torque about C produced by firing the thruster is $\bar{M}_T$. In this model, the torque exerted by the RMS on the shuttle at A will have only one component (in the $\bar{j}$ direction).

The angular velocity of the shuttle at any time, $\bar{\omega}$, can be written in component form as

$$\bar{\omega}_s = p_s\bar{i} + q_s\bar{j} + r_s\bar{k}$$

For the two-dimensional model, this reduces to

$$\bar{\omega} = q_s\bar{j}$$

The force and moment equations for the shuttle in body-fixed coordinates are (for the two-dimensional model)

$$\Sigma F_x = T_x + A_x = m_x(\dot{u} + q_s w) \qquad \text{(II.1)}$$

$$\Sigma F_z = T_z + A_z = m_x(\dot{w} - q_s u) \qquad \text{(II.2)}$$

$$\Sigma M_C = M_A + r_{CA} \times A_x + M_T =$$
$$M_A + z_{CA}A_x - x_{CA}A_z + M_T =$$
$$I_{yys}\dot{q}_s \qquad \text{(II.3)}$$

where m_s is the mass of the shuttle and I_{yys} is the mass moment of inertia of the shuttle about the y axis (through C).

From equations (II.1),(II.2), and (II.3), we get

$$\dot{u} = -q_s w + \frac{T_x + A_x}{m_s} \tag{II.4}$$

$$\dot{w} = q_s u + \frac{T_z + A_z}{m_s} \tag{II.5}$$

$$\dot{q}_s = \frac{1}{I_{yys}} \{M_A + z_{CA}A_x - x_{CA}A_z + M_T\} \tag{II.6}$$

Equations (II.4), (II.5), and (II.6) would give the shuttle c.g. center of mass velocity and pitch rate versus time if they could be intetrated. However, A_x, A_z, and M_A are unknown.

In order to determine A_x, A_z, and M_A, it is necessary to consider the payload/RMS as a second rigid body and look at its motion. Let D be the center of mass of the payload/RMS combination. The shuttle/payload/RMS is shown in Figure II.1 below, while the payload/RMS free-body diagram is shown in Figure II.3.

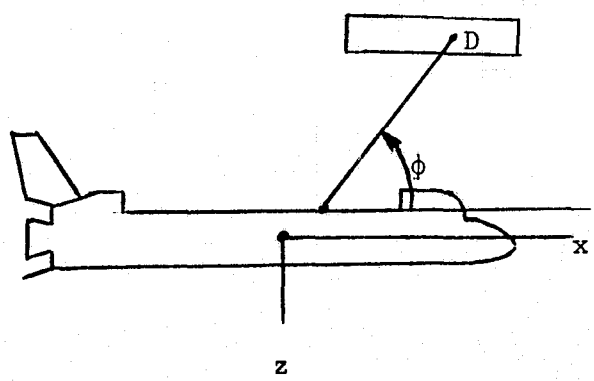

Figure II.2: Definition of ϕ

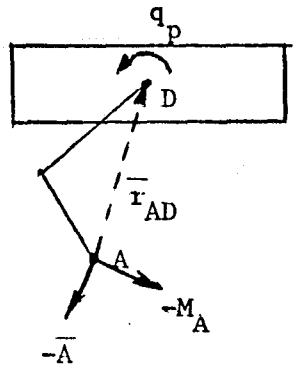

Figure II.3: Arm-Payload Geometry

The equations of motion for the payload/RMS are

$$\Sigma F_x = -A_x = m_p a_{D_x} \tag{II.7}$$

$$\Sigma F_y = -A_z = m_p a_{D_z} \tag{II.8}$$

$$\Sigma M_D = -M_T + \bar{r}_{DA} \times (-\bar{A}) = I_{yy_p} \dot{q}_p \tag{II.9}$$

where m_p is the mass of the payload/RMS combination and I_{yy_p} is its mass moment of inertia about an axis parallel to the y-axis through point D.

Note that in equations (II.7) and (II.8), a_{D_x} and a_{D_z} are expressed in terms of a rotating coordinate system which is rotating at the angular rate of the shuttle (i.e., $\bar{\Omega}_{coords} = \bar{\omega}_s = q_s \bar{j}$).

From Figure (II.2), note that

$$\bar{r}_{AD} = d \cos \phi \, \bar{i} - d \sin \phi \, \bar{k} \tag{II.10}$$

where ϕ is the angle between the positive x-axis and the line AD, and d is the distance from A to D. Thus, $\bar{r}_{CD}$ is given by

$$\bar{r}_{CD} = \bar{r}_{CA} + \bar{r}_{AD}$$

$$= (x_{CA} + d \cos \phi)\bar{i} + (z_{CA} - d \sin \phi)\bar{k} \tag{II.11}$$

The quantity d can be allowed to vary during relative motion of the shuttle and payload. The present analysis will allow this and it will be assumed that this motion is known over the period of interest and will be specified over the period of interest by three parameters, d_o, $\dot{d}_o$, and $\ddot{d}_o$. The motion will be modeled as

$$d(t) = d_o + \dot{d}_o t + \ddot{d}_o t^2/2 \qquad \text{(II.12)}$$

The quantities d_o, $\dot{d}_o$, and $\ddot{d}_o$ will be input parameters in the computer program.

It is now necessary to develop expressions for a_{D_x} and a_{D_y}. In general,

$$\bar{a}_D = \bar{a}_C + \bar{a}_{D_{rel}} + \bar{\Omega} \times (\bar{\Omega} \times \bar{r}_{CD}) + 2\bar{\Omega} \times \bar{V}_{D_{rel}} + \dot{\bar{\Omega}} \times \bar{r}_{CD} \qquad \text{(II.13)}$$

It is most convenient to develop each term of equation (II.13) separately and then combine them to form $\bar{a}_D$. In this manner, errors can be more easily avoided.

First, $\bar{a}_C$ is known from equations (II.1) and (II.2), i.e.,

$$\bar{a}_C = (\dot{u} + q_s w)\,\bar{i} + (\dot{w} - q_s u)\,\bar{k} \qquad \text{(II.14)}$$

The quantity $\bar{a}_{D_{rel}}$ is the acceleration of point D relative to point C disregarding coordinate rotation. Thus, $\bar{a}_{D_{rel}}$ is the second derivative of $\bar{r}_{CD}$ taken with unit vectors fixed. (It is convenient to do this in two steps as the first derivative will be identified as $\bar{V}_{D_{rel}}$ and will be used in a later term).

Equation (II.11) gives $\bar{r}_{CD}$. Thus,

$$\bar{V}_{D_{rel}} = (+\dot{d}\cos\phi - d\dot{\phi}\sin\phi)\bar{i} + (-\dot{d}\sin\phi - d\dot{\phi}\cos\phi)\bar{k} \qquad \text{(II.15)}$$

since x_{CA} and z_{CA} are constant. Next,

$$\bar{a}_{D_{rel}} = (+\ddot{d}\cos\phi - 2\dot{d}\dot{\phi}\sin\phi - d\ddot{\phi}\sin\phi - d\dot{\phi}^2\cos\phi)\bar{i}$$
$$+ (-\ddot{d}\sin\phi - 2\dot{d}\dot{\phi}\cos\phi - d\ddot{\phi}\cos\phi + d\dot{\phi}^2\sin\phi)\bar{k} \qquad \text{(II.16)}$$

The quantity $\bar{\Omega} \times (\bar{\Omega} \times \bar{r}_{CD})$ is given by

$$q_s \bar{j} \times [q_s\bar{j} \times \{(x_{CA} + d\cos\phi)\bar{i} + (z_{CA} - d\sin\phi)\bar{k})\}]$$

Thus,

$$\bar{\Omega} \times (\bar{\Omega} \times \bar{r}_{CD}) = (-q_s^2 x_{CA} - q_s^2 d\cos\phi)\bar{i}$$
$$+ (-q_s^2 z_{CA} + q_s^2 d\sin\phi)\bar{k} \qquad \text{(II.17)}$$

The term $2\bar{\Omega} \times \bar{V}_{D_{rel}}$ is given by

$$2\bar{\Omega} \times \bar{V}_{D_{rel}} = 2q_s\bar{j} \times \{(+\dot{d}\cos\phi - d\dot{\phi}\sin\phi)\bar{i}$$
$$+ (-\dot{d}\sin\phi - d\dot{\phi}\cos\phi)\bar{k}\}$$

Thus,

$$2\bar{\Omega} \times \bar{V}_{D_{rel}} = (-2q_s\dot{d}\sin\phi - 2q_s d\dot{\phi}\cos\phi)\bar{i}$$
$$+ (-2q_s\dot{d}\cos\phi + 2q_s d\dot{\phi}\sin\phi)\bar{k} \qquad \text{(II.18)}$$

Finally, the term $\dot{\bar{\Omega}} \times \bar{r}_{CD}$ is given by

$$\dot{\bar{\Omega}} \times \bar{r}_{CD} = \dot{q}_s\bar{j} \times \{(x_{CA} + d\cos\phi)\bar{i} + (z_{CA} - d\sin\phi)\bar{k}\}$$

Thus,

$$\dot{\bar{\Omega}} \times \bar{r}_{CD} = (\dot{q}_s z_{CA} - \dot{q}_s d \sin\phi)\bar{i} + (-\dot{q}_s x_{CA} - \dot{q}_s d \cos\phi)\bar{k} \qquad \text{(II.19)}$$

Combination of equations (II.14), (II.15), (II.18), and (II.19) results in

$$\begin{aligned} a_{D_x} &= \dot{u} + q_s w + \ddot{d} \cos\phi - 2\dot{d}\dot{\phi} \sin\phi \\ &\quad - d\ddot{\phi} \sin\phi - d\dot{\phi}^2 \cos\phi - q_s^2 x_{CA} \\ &\quad - q_s^2 d \cos\phi - 2q_s \dot{d} \sin\phi \\ &\quad - 2q_s d\dot{\phi} \cos\phi + \dot{q}_s z_{CA} \\ &\quad - \dot{q}_s d \sin\phi \end{aligned} \qquad \text{(II.20)}$$

$$\begin{aligned} a_{D_z} &= \dot{w} - q_s u - \ddot{d} \sin\phi - 2\dot{d}\dot{\phi} \cos\phi \\ &\quad - d\ddot{\phi} \cos\phi + d\dot{\phi}^2 \sin\phi - q_s^2 z_{CA} \\ &\quad + q^2 d \sin\phi - 2q_s \dot{d} \cos\phi \\ &\quad + 2q_s d\dot{\phi} \sin\phi - \dot{q}_s x_{CA} \\ &\quad - \dot{q}_s d \cos\phi \end{aligned} \qquad \text{(II.21)}$$

Finally, the quantity q_p can be related to q_s by

$$q_p = q_s + \dot{\phi} \qquad \text{(II.22)}$$

and

$$\dot{q}_p = \dot{q}_s + \ddot{\phi} \qquad \text{(II.23)}$$

The procedure now will be to introduce the expressions derived for a_{D_x}, a_{D_y}, and q_p into equations (II.7), (II.8), and II.9) in order to develop expressions for A_x, A_y, and and a differential equation for $\ddot{\phi}$.

Equation (II.7) becomes

$$-\frac{A_x}{m_p} = \dot{u} + \dot{q}_s\,(z_{CA} - d\sin\phi) + q_s\,(w - 2\dot{d}\sin\phi - 2d\dot{\phi}\cos\phi) + (+\ddot{d}\cos\phi - 2\dot{d}\dot{\phi}\sin\phi - d\dot{\phi}^2\cos\phi) + q_s^2\,(-x_{CA} - d\cos\phi) + \ddot{\phi}(-d\sin\phi) \qquad \text{(II.24)}$$

Similarly, equation (II.8) becomes

$$-\frac{A_z}{m_p} = \dot{w} + \dot{q}_s\,(-x_{CA} - d\cos\phi) + q_s\,(-u - 2\dot{d}\cos\phi + 2d\dot{\phi}\sin\phi) + (-\ddot{d}\sin\phi - 2\dot{d}\dot{\phi}\cos\phi + d\dot{\phi}^2\sin\phi) + q_s^2\,(-z_{CA} + d\sin\phi) + \ddot{\phi}(-d\cos\phi) \qquad \text{(II.25)}$$

Equation (II.9) becomes

$$-M_A - A_z\,d\cos\phi - A_x\,d\sin\phi = I_{yys}\,\dot{q}_s + I_{yyp}\,\ddot{\phi} \qquad \text{(II.26)}$$

Equations (II.1), (II.2), (II.3), and (II.26) are a set of four simultaneous first order differential equations in the four variables u, w, q_s, and $\dot{\theta}$. However, they are not in a form amenable to numerical integration and equations

(II.24) and (II.25) must be used along with considerable algebraic manipulation to put them in such a form. In order to simplify this process, the following definitions are made.

$$
\begin{aligned}
b_1 &= m_p(z_{CA} - d\sin\phi) \\
b_2 &= -m_p(d\sin\phi) \\
b_3 &= \{q_s(w - 2\dot{d}\sin\phi - 2d\dot{\phi}\cos\phi) \\
&\quad + (\ddot{d}\cos\phi - 2\dot{d}\dot{\phi}\sin\phi - 2d\dot{\phi}^2\cos\phi) \\
&\quad + q_s^2(-x_{CA} - d\cos\phi)\}\, m_p
\end{aligned}
\tag{II.27}
$$

With these definitions, equation (II.24) becomes

$$
-A_x = m_p\dot{u} + b_1\dot{q}_s + b_2\ddot{\phi} + b_3 \tag{II.28}
$$

Substitution of this into equation (II.1) results in

$$
T_x - m_p\dot{u} - b_1\dot{q}_s - b_2\ddot{\phi} - b_3 = m_s\dot{u} + m_s q_s w \tag{II.29}
$$

Equation (II.29) can be rewritten as

$$
(m_s + m_p)\,\dot{u} + 0\,\dot{w} + b_1\dot{q}_s + b_2\ddot{\phi} = T_x - m_s q_s w - b_3 \tag{II.30}
$$

In a similar manner, the definitions

$$C_1 = (-x_{CA} - d\cos\phi)m_p$$

$$C_2 = m_p(-d\cos\phi)$$

$$C_3 = \{(-u - 2\dot{d}\cos\phi + 2d\dot{\phi}\sin\phi)q_s + (-\ddot{d}\sin\phi - 2\dot{d}\dot{\phi}\cos\phi + d\dot{\phi}^2\sin\phi) + q_s^2(-z_{CA} + d\sin\phi)\}m_p \quad \text{(II.31)}$$

lead to rewriting equation (II.25) in the form

$$-A_z = m_p\dot{w} + C_1\dot{q}_s + C_2\ddot{\phi} + C_3 \quad \text{(II.32)}$$

Substitution of equation (II.32) into equation (II.2) results in

$$T_z - m_p\dot{w} - C_1\dot{q}_s - C_2\ddot{\phi} - C_3 = m_s\dot{w} - m_s q_s u$$

or

$$0\,\dot{u} + (m_s + m_p)\dot{w} + C_1\dot{q}_s + C_2\ddot{\phi} = T_z - C_3 + m_s q_s u \quad \text{(II.33)}$$

Next, it is necessary to substitute equation (II.28) and (II.32) into equation (II.3). However, prior to this step, let us assume that M_A is of the form

$$M_A = K(\phi - \phi_o) + C\dot{\phi} \quad \text{(II.34)}$$

This will make equation (II.3) and (II.9) independent so that neither has to be used to solve for M_A to substitute into the other. With the indicated substitutions, equation (II.3) becomes

$$M_A - z_{CA}m_p\dot{u} - z_{CA}b_1\dot{q}_s - z_{CA}b_2\ddot{\phi}$$

$$- z_{CA}b_3 + x_{CA}m_p\dot{w} + x_{CA}c_1\dot{q}_s \qquad \text{(II.35)}$$

$$+ x_{CA}c_2\ddot{\phi} + x_{CA}C_3 + M_T = I_{yys}\dot{q}_s$$

Regrouping the terms in equation (II.35) leads to

$$(z_{CA}m_p)\dot{u} + (I_{yyx} + z_{CA}b_1 - x_{CA}C_1)\dot{q}_s$$

$$+ (- x_{CA}m_p)\dot{w} + (z_{CA}b_2 - x_{CA}C_2)\ddot{\phi} \qquad \text{(II.36)}$$

$$= M_T + M_A + x_{CA}C_3 - z_{CA}b_3$$

Substitution of equation (II.28) and (II.32) into equation (II.26) yields

$$- M_A + (m_p d\cos\phi)\dot{w} + (C_1 d\cos\phi)\dot{q}_s$$

$$+ (C_2 d\cos\phi)\ddot{\phi} + C_3 d\cos\phi$$

$$+ (m_p d\sin\phi)\dot{u} + (b_1 d\sin\phi)\dot{q}_s$$

$$+ (b_2 d\sin\phi)\ddot{\phi} + b_3 d\sin\phi$$

$$= I_{yyp}\dot{q}_s + I_{yyp}\ddot{\phi} \qquad \text{(II.37)}$$

Collection of terms in equation (II.37) results in

$$(-m_p d \sin\phi)\dot{u} + (-m_p d \cos\phi)\dot{w}$$

$$+ (I_{yyp} - b_1 d \sin\phi - C_1 d \cos\phi)\dot{q}_s$$

$$+ (I_{yyp} - C_2 d \cos\phi - b_2 d \sin\phi)\ddot{\phi} =$$

$$- M_A + C_3 d \cos\phi + b_3 d \sin\phi \qquad \text{(II.38)}$$

Equations (II.30), (II.33), (II.36), and (II.38) are now of the form

$$\begin{aligned}
B_{11}\dot{u} + B_{12}\dot{w} + B_{13}\dot{q}_s + B_{14}\ddot{\phi} &= D_1 \\
B_{21}\dot{u} + B_{22}\dot{w} + B_{23}\dot{q}_s + B_{24}\ddot{\phi} &= D_2 \\
B_{31}\dot{u} + B_{32}\dot{w} + B_{33}\dot{q}_s + B_{34}\ddot{\phi} &= D_3 \\
B_{41}\dot{u} + B_{42}\dot{w} + B_{43}\dot{q}_s + B_{44}\ddot{\phi} &= D_4
\end{aligned} \qquad \text{(II.39)}$$

where

$B_{11} = m_p + m_s$
$B_{12} = 0$
$B_{13} = b_1$
$B_{14} = b_2$
$D_1 = T_x - m_s q_s w - b_3$

$B_{21} = 0$
$B_{22} = (m_p + m_s)$
$B_{23} = C_1$
$B_{24} = C_2$
$D_2 = T_z + m_s q_s u - C_3$

$B_{31} = z_{CA} m_p$
$B_{32} = -x_{CA} m_p$
$B_{33} = I_{yys} + z_{CA} b_1 - x_{CA} C_1$
$B_{34} = z_{CA} b_2 - x_{CA} C_2$
$D_3 = M_T + M_A + x_{CA} C_3 - z_{CA} b_3$

$B_{41} = -m_p d \sin\phi$
$B_{42} = -m_p d \cos\phi$
$B_{43} = I_{yys} - b_1 d \sin\phi - C_1 d \cos\phi$
$B_{44} = I_{yyp} - c_2 d \cos\phi - b_2 d \sin\phi$
$D_4 = -M_A + C_3 d \cos\phi + b_3 d \sin\phi$

The differential equations of motion for the system can be written as (let $\ddot{\theta} = \dot{\omega}$)

$$\begin{Bmatrix} & & \\ & B & \\ & & \end{Bmatrix} \begin{Bmatrix} \dot{u} \\ \dot{w} \\ \dot{q}_s \\ \dot{\omega} \end{Bmatrix} = \begin{Bmatrix} D_1 \\ D_2 \\ D_3 \\ D_4 \end{Bmatrix} \qquad \text{(II.40)}$$

plus the equation

$$\dot{\theta} = \omega \qquad \text{(11.41)}$$

Using a linear systems solver or matrix inverse at each derivative evaluation, the vector

$$\begin{Bmatrix} \dot{u} \\ \dot{w} \\ \dot{q}_s \\ \dot{\omega} \\ \dot{\theta} \end{Bmatrix}$$

can be formed.

Given initial conditions

$$\begin{Bmatrix} u \\ w \\ \dot{q}_s \\ \dot{\omega} \\ \dot{\theta} \end{Bmatrix} = \begin{Bmatrix} 0 \\ 0 \\ 0 \\ 0 \\ 0 \end{Bmatrix} ,$$

an initial value for θ, i.e., θ_o, values for d, $\dot{d}$, and $\ddot{d}$, m_p, m_s, I_{yys}, I_{yyp}, the spring constant K, the geometric quantities $\bar{r}_{CA}$ (x_{CA} and z_{CA}) $\bar{r}_{CT}$ (x_{CT} and z_{CT}), and the thrust components T_x and T_z, then it is possible to carry out the required numerical integration.

As the integration is carried out, A_x, A_z, and m can be evaluated at each point in time from equations (II.28), (II.32), and (II.34), respectively.

III. TWO JOINT MODEL

In the two joint model, single axis pin joints will be assumed at the shoulder and the wrist of the shuttle/arm/payload combination.

The forces and moments acting on the shuttle itself are shown below in Figure III.1.

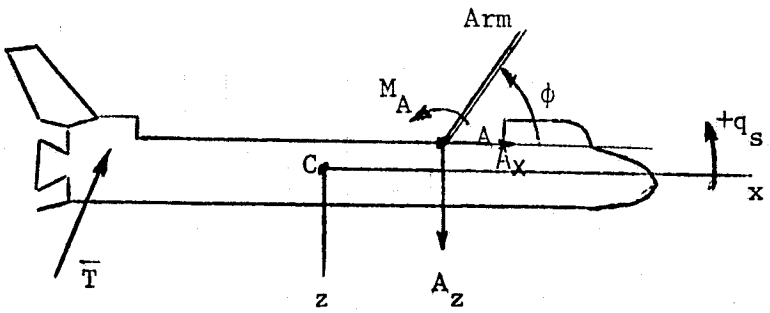

Figure III.1: Shuttle Free-Body Diagram

where

$$\bar{T} = T_x\bar{i} + \cancel{T_y\bar{j}}^{0} + T_z\bar{k}$$

$$\bar{A} = A_x\bar{i} + \cancel{A_y\bar{j}}^{0} + A_z\bar{k}$$

$$\bar{V}_c = u\,\bar{i} + \cancel{v\,\bar{j}}^{0} + w\,\bar{k}$$

$$\bar{r}_{CA} = x_{CA}\bar{i} + \cancel{y_{CA}\bar{j}}^{0} + z_{CA}\bar{k}$$

$$\bar{M}_A = \cancel{L_A\bar{i}}^{0} + M_A\bar{j} + \cancel{N_A\bar{k}}^{0}$$

$$\bar{M}_T = \cancel{L_T\bar{i}}^{0} + M_T\bar{j} + \cancel{N_T\bar{k}}^{0}$$

$$\bar{\omega}_s = \cancel{p_s\bar{i}}^{0} + q_s\bar{j} + \cancel{r_s\bar{k}}^{0}$$

The quantities marked through are zero because the model is two-dimensional. The xyz coordinate system is centered at the shuttle center of mass, C, and rotates with the shuttle.

The force and moment equations for the shuttle in body fixed axes are, as before [see equations (II.1 thru II.3)].

$$\Sigma F_x = T_x + A_x = m_s(\dot{u} + q_s w) \tag{III.1}$$

$$\Sigma F_y = T_y + A_y = m_s(\dot{w} - q_s u) \tag{III.2}$$

$$\Sigma M_C = M_A + M_T + z_{CA}A_x - x_{CA}A_z = I_{yys}\dot{q}_s \tag{III.3}$$

where all variables are defined as they were in the analysis of the single joint model.

Equations (III.1) through (III.3) can be written as differential equations for $\dot{u}$, $\dot{w}$, and $\dot{q}_s$ with unknowns A_x, A_z, and M_A appearing on the right hand sides. Thus,

$$\dot{u} = -q_s w + \frac{T_x}{m_s} + \frac{A_x}{m_s} \tag{III.4}$$

$$\dot{w} = q_s u + \frac{T_z}{m_s} + \frac{A_z}{m_s} \tag{III.5}$$

$$\dot{q}_s = \frac{1}{I_{yys}} \{M_T + z_{CA}A_x - x_{CA}A_z + M_A\} \tag{III.6}$$

As before, the torque exerted by the arm on the shuttle at point A will be modeled as

$$M_A = K(\phi - \phi_0) + C\dot{\phi} \tag{III.7}$$

In order to find the forces A_x and A_z, it is necessary to consider the arm and then the payload.

The arm will be assumed to be massless. Thus, its effect is to transmit and modify torques. The free-body diagram of the arm is shown in Figure III.2.

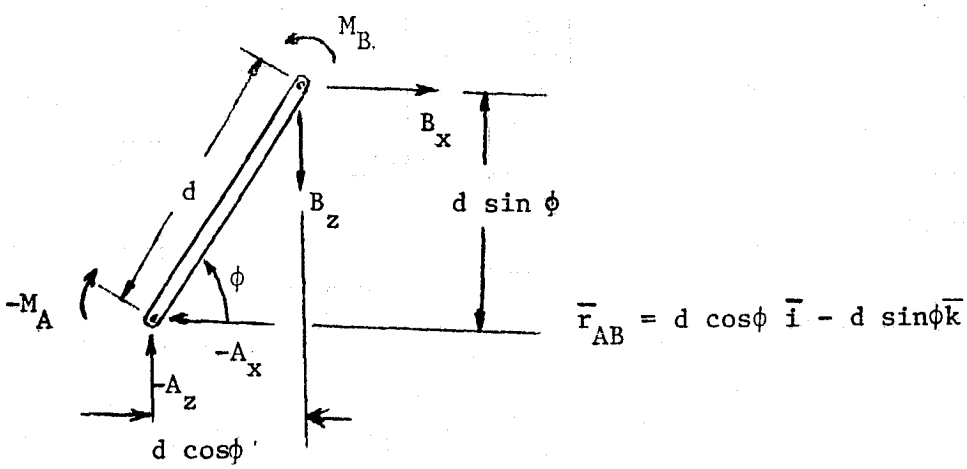

Figure III.2: Arm Free-Body Diagram

The equations of motion for the arm are

$$\Sigma F_x = -A_x + B_x = 0 \qquad \text{(III.8)}$$

$$\Sigma F_y = -A_z + B_z = 0 \qquad \text{(III.9)}$$

$$\Sigma M_A = -M_A + M_B - B_z d \cos\phi - B_x d \sin\phi = 0 \qquad \text{(III.10)}$$

From equations (III.8) through (III.10), we get

$$A_x = B_x \qquad \text{(III.11)}$$

$$A_z = B_z \qquad \text{(III.12)}$$

$$M_B = M_A + A_z d \cos\phi + A_x d \sin\phi \qquad \text{(III.13)}$$

However, as was the case with the shoulder joint, a form will subsequently be specified for M_B (in terms of an angle yet to be defined).

The next step is to examine the free-body diagram of the payload shown below

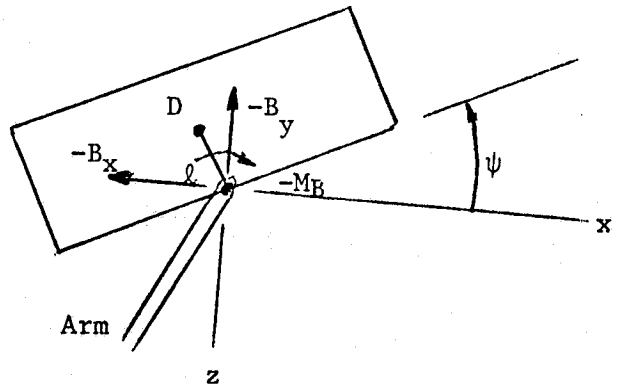

Figure III.3: Payload Free-Body Diagram

The equations of motion for the payload are given by

$$\Sigma F_x = -B_x = m_p\, a_{D_x} = -A_x \tag{III.14}$$

$$\Sigma F_z = -B_z = m_p\, a_{D_z} = -A_z \tag{III.15}$$

$$\Sigma \bar{M}_D = -M_B \bar{j} + \bar{r}_{DB} \times (-\bar{B}) = I_{yyp}\, \dot{q}_p \bar{j} \tag{III.16}$$

where

$$\bar{r}_{DB} = -\bar{r}_{BD} = +\ell \sin\psi\, \bar{i} + \ell \cos\psi\, \bar{k}$$

$$\bar{r}_{DB} \times (-\bar{B}) = \bar{r}_{BD} \times \bar{B}$$

$$= \bar{r}_{BD} \times \bar{A}$$

$$= (-\ell \sin\psi \bar{i} - \ell \cos\psi\, \bar{k}) \times (A_x \bar{i} + A_z \bar{k})$$

$$\bar{r}_{DB} \times (-\bar{B}) = (+ A_z \ell \sin\psi - A_x \ell \cos\psi)\bar{j}$$

Thus, equation (III.16) can be written as

$$\Sigma M_D = -M_B + A_z \ell\sin\psi - A_x \ell\cos\psi = I_{yyp}\dot{q}_p \qquad \text{(III.17)}$$

In equations (III.14) and (III.15), a_{D_x} and a_{D_z} are expressed in a coordinate system which rotates with the shuttle (at an angular rate given by $\bar{\Omega} = \bar{\omega}_s = q_s\bar{j}$).

As before [see equation (II.13)]

$$\bar{a}_D = \bar{a}_C + \bar{a}_{D_{rel}} + \bar{\Omega} \times (\bar{\Omega} \times \bar{r}_{CD}) + 2\bar{\Omega} \times \bar{V}_{rel} + \dot{\bar{\Omega}} \times \bar{r}_{CD} \qquad \text{(III.18)}$$

In order to generate a complete expression for $\bar{a}_D$, it is necessary to first write an explicit form for $\bar{r}_{CD}$. Thus,

$$\bar{r}_{CD} = \bar{r}_{CA} + \bar{r}_{AB} + \bar{r}_{BD}$$

or

$$\bar{r}_{CD} = (x_{CA} + d\cos\phi - \ell\sin\psi)\,\bar{i} + (z_{CA} - d\sin\phi - \ell\cos\psi)\bar{k} \qquad \text{(III.19)}$$

As in the single joint model, the length of the arm will be modeled as

$$d(t) = d_o + \dot{d}_o\, t + \ddot{d}_o t^2/2 \qquad \text{(III.20)}$$

where d_o, $\dot{d}_o$, and $\ddot{d}$ are input parameters. Now let us proceed to develop each of the terms of the right-hand side of equation (III.18) individually.

From equations (III.1) and (III.2), $\bar{a}_c$ is given by

$$\bar{a}_c=(\dot{u} + q_s\, w)\bar{i} + (\dot{w} - q_s u)\bar{k} \qquad \text{(III.21)}$$

Next, the quantities $\bar{V}_{D_{rel}}$ and $\bar{a}_{D_{rel}}$ will be developed from $\bar{r}_{CD}$. Recall that $\bar{r}_{CD}$ is given by

$$\bar{r}_{CD} = (x_{CA} + d\cos\phi - \ell\sin\psi)\bar{i} + (z_{CA} - d\sin\phi - \ell\cos\psi)\bar{k} \qquad \text{(III.22)}$$

where x_{CA}, z_{CA}, and ℓ are constants. To find $\bar{V}_{D_{rel}}$ and $\bar{a}_{D_{rel}}$, $\bar{i}$ and $\bar{k}$ are treated as constant vectors also. Thus,

$$\bar{V}_{D_{rel}} = (\dot{d}\cos\phi - d\dot{\phi}\sin\phi - \ell\dot{\psi}\cos\psi)\bar{i} + (-\dot{d}\sin\phi - d\dot{\phi}\cos\phi + \ell\dot{\psi}\sin\psi)\bar{k} \qquad \text{(III.23)}$$

and

$$\begin{aligned}\bar{a}_{D_{rel}} = {} & (\ddot{d}\cos\phi - 2\dot{d}\dot{\phi}\sin\phi - d\ddot{\phi}\sin\phi - d\dot{\phi}^2\cos\phi - \ell\ddot{\psi}\cos\psi + \ell\dot{\psi}^2\sin\psi)\bar{i} \\ & + (-\ddot{d}\sin\phi - 2\dot{d}\dot{\phi}\cos\phi - d\ddot{\phi}\cos\phi + d\dot{\phi}^2\sin\phi + \ell\ddot{\psi}\sin\psi + \ell\dot{\psi}^2\cos\psi)\bar{k}\end{aligned} \qquad \text{(III.24)}$$

The quantity $\bar{\Omega} \times (\bar{\Omega} \times \bar{r}_{CD})$ is given by

$$q_s\bar{j} \times [q_s\bar{j} \times \{(x_{CA} + d\cos\phi - \ell\sin\psi)\bar{i} + (z_{CA} - d\sin\phi - \ell\cos\psi)\bar{k}\}]$$

Thus,

$$\begin{aligned}\bar{\Omega} \times (\bar{\Omega} \times \bar{r}_{CD}) = {} & (-q_s^2 x_{CA} - q_s^2 d\cos\phi + q_s^2\ell\sin\psi)\bar{i} \\ & + (-q_s^2 z_{CA} + q_s^2 d\sin\phi + q_s^2\ell\cos\psi)\bar{k}\end{aligned} \qquad \text{(III.25)}$$

The term $2\bar{\Omega} \times \bar{V}_{rel}$ is generated from

$$\begin{aligned}2\bar{\Omega} \times \bar{V}_{rel} = {} & 2q_s\bar{j} \times \{(\dot{d}\cos\phi - d\dot{\phi}\sin\phi - \ell\dot{\psi}\cos\psi)\bar{i} \\ & + (-\dot{d}\sin\phi - d\dot{\phi}\cos\phi + \ell\dot{\psi}\sin\psi)\}\bar{k}\end{aligned}$$

and

$$2\bar{\Omega} \times \bar{V}_{rel} = (-2q_s\dot{d}\sin\phi - 2q_s d\dot{\phi}\cos\phi + 2q_s \ell\dot{\psi}\sin\psi)\bar{i}$$
$$+ (-2q_s\dot{d}\cos\phi + 2q_s d\dot{\phi}\sin\phi + 2q_s \ell\dot{\psi}\cos\psi)\bar{k} \qquad \text{(III.26)}$$

Finally, the $\dot{\bar{\Omega}} \times \bar{r}_{CD}$ term is generated by

$$\dot{\bar{\Omega}} \times \bar{r}_{CD} = \dot{q}_s\bar{j} \times \{(x_{CA} + d\cos\phi - \ell\sin\psi)\bar{i}$$
$$+ (z_{CA} - d\sin\phi - \ell\cos\psi)\bar{k}$$

or

$$\dot{\bar{\Omega}} \times \bar{r}_{CD} = (\dot{q}_s z_{CA} - \dot{q}_s d\sin\phi - \dot{q}_s \ell\cos\psi)\bar{i}$$
$$+ (-\dot{q}_s x_{CA} - \dot{q}_s d\cos\phi + \dot{q}_s \ell\sin\psi)\bar{k} \qquad \text{(III.27)}$$

Combination of Equations (III.21), (III.24), (III.25), (III.26), and (III.27) to form $\bar{a}_D$ results in

$$a_{D_x} = \dot{u} + q_s w + \ddot{d}\cos\phi - 2\dot{d}\dot{\phi}\sin\phi - d\ddot{\phi}\sin\phi$$
$$- d\dot{\phi}^2\cos\phi - \ell\ddot{\psi}\cos\psi + \ell\dot{\psi}^2\sin\psi$$
$$- q_s^2 x_{CA} - q_s^2 d\cos\phi + q_s^2 \ell\sin\psi$$
$$- 2q_s\dot{d}\sin\phi - 2q_s\dot{\phi}\cos\phi + 2q_s\ell\dot{\psi}\sin\psi$$
$$+ \dot{q}_s z_{CA} - \dot{q}_s d\sin\phi - \dot{q}_s\ell\cos\psi \qquad \text{(III.28)}$$

$$a_{D_z} = \dot{w} - q_s u - \ddot{d}\sin\phi - 2\dot{d}\dot{\phi}\cos\phi - d\ddot{\phi}\cos\phi$$
$$+ d\dot{\phi}^2\sin\phi + \ell\ddot{\psi}\sin\psi + \ell\dot{\psi}^2\cos\psi$$
$$- q_s^2 z_{CA} + q_s^2 d\sin\phi + q_s^2\ell\cos\psi$$
$$- 2q_s\dot{d}\cos\phi + 2q_s d\dot{\phi}\sin\phi + 2q_s\ell\dot{\psi}\cos\psi$$
$$- \dot{q}_s x_{CA} - \dot{q}_s d\cos\phi + \dot{q}_s\ell\sin\psi \qquad \text{(III.29)}$$

Substituting equations (III.28) and (III.29) into equations (III.14) and (III.15) and collecting terms, we get

$$
\begin{aligned}
-A_x = {} & m_p\dot{u} + 0\,\dot{w} \\
& + m_p(z_{CA} - d\sin\phi - \ell\cos\psi)\dot{q}_s \\
& + m_p(-d\sin\phi)\ddot{\phi} + m_p(-\ell\cos\psi)\ddot{\psi} \\
& + m_p[q_s^2(-x_{CA} - d\cos\phi + \ell\sin\psi) \\
& \quad + (\ddot{d}\cos\phi - 2\dot{d}\dot{\phi}\sin\phi - d\dot{\phi}^2\cos\phi + \ell\dot{\psi}^2\sin\psi) \\
& \quad + q_s(w - 2\dot{d}\sin\phi - 2d\dot{\phi}\cos\phi + 2\ell\dot{\psi}\sin\psi)]
\end{aligned}
\qquad \text{(III.30)}
$$

and

$$
\begin{aligned}
-A_z = {} & 0\,\dot{u} + m_p\,\dot{w} \\
& + m_p(-x_{CA} - d\cos\phi + \ell\sin\psi)\dot{q}_s \\
& + m_p(-d\cos\phi)\ddot{\phi} + m_p(\ell\sin\psi)\ddot{\psi} \\
& + m_p[q_s^2(-z_{CA} + d\sin\phi + \ell\cos\psi) \\
& \quad + (-\ddot{d}\sin\phi - 2\dot{d}\dot{\phi}\cos\phi + d\dot{\phi}^2\sin\phi + \ell\dot{\psi}^2\cos\psi) \\
& \quad + q_s(-u - 2\dot{d}\cos\phi + 2d\dot{\phi}\sin\phi + 2\ell\dot{\psi}\cos\psi)]
\end{aligned}
\qquad \text{(III.31)}
$$

With the definitions below, the expressions for A_x and A_z can be greatly simplified.

$$
\begin{aligned}
b_1 &= (z_{CA} - d\sin\phi - \ell\cos\psi)m_p \\
b_2 &= m_p(-d\sin\phi) \\
b_3 &= m_p[q_s(w - 2\dot{d}\sin\phi - 2d\dot{\phi}\cos\phi + 2\ell\dot{\psi}\sin\psi) \\
&\quad + (\ddot{d}\cos\phi - 2\dot{d}\dot{\phi}\sin\phi - d\dot{\phi}^2\cos\phi + \ell\dot{\psi}^2\sin\psi) \\
&\quad + q_s^2(-x_{CA} - d\cos\phi + \ell\sin\psi)] \\
b_4 &= m_p(-\ell\cos\psi)
\end{aligned}
\qquad \text{(III.32)}
$$

$$c_1 = (-x_{CA} - d\cos\phi + \ell\sin\psi)m_p$$

$$c_2 = m_p(-d\cos\phi)$$

$$c_3 = m_p\,[q_s(-u - 2\dot{d}\cos\varphi + 2d\dot{\phi}\sin\phi + 2\ell\dot{\psi}\cos\psi)$$
$$+ (-\ddot{d}\sin\phi - 2\dot{d}\dot{\phi}\cos\phi + d\dot{\phi}^2\sin\phi + \ell\dot{\psi}^2\cos\psi)$$
$$+ q_s^2(-z_{CA} + d\sin\phi + \ell\cos\psi)]$$

$$c_4 = m_p(\ell\sin\psi) \qquad \text{(III.33)}$$

The resulting expressions for A_x and A_z are

$$-A_x = m_p\dot{u} + b_1\dot{q}_s + b_2\ddot{\phi} + b_4\ddot{\psi} + b_3 \qquad \text{(III.34)}$$

$$-A_z = m_p\dot{w} + c_1\dot{q}_s + c_2\ddot{\phi} + c_4\ddot{\psi} + c_3 \qquad \text{(III.35)}$$

Rewriting equations (III.1) and (III.2), we have

$$m_s\dot{u} - A_x = T_x - m_s q_s w \qquad \text{(III.36)}$$

$$m_s\dot{w} - A_z = T_z + m_s q_s u \qquad \text{(III.37)}$$

Combination of equations (III.34) and (III.36), (III.35) and (III.37), results in

$$(m_s + m_p)\dot{u} + b_1\dot{q}_s + b_2\ddot{\phi} + b_4\ddot{\psi} = T_x - m_s q_s w - b_3 \qquad \text{(III.38)}$$

$$(m_s + m_p)\dot{w} + c_1\dot{q}_s + c_2\ddot{\phi} + c_4\ddot{\psi} = T_z = m_s q_s u - c_3 \qquad \text{(III.39)}$$

Equations (III.3) can be rewritten as

$$I_{yys}\dot{q}_s + x_{CA}A_z - z_{CA}A_x = M_T + M_A \qquad \text{(III.40)}$$

Combination of equations (III.34), (III.35), and (III.40) results in

$$I_{yys}\dot{q}_s - x_{CA}m_p\dot{w} - x_{CA}c_1\dot{q}_s - x_{CA}c_2\ddot{\phi}$$

$$-x_{CA}c_A\ddot{\psi} - x_{CA}c_3 + z_{CA}m_p\dot{u} + z_{CA}b_1\dot{q}_s$$

$$+z_{CA}b_2\ddot{\phi} + z_{CA}b_4\ddot{\psi} + z_{CA}b_3 = M_T + M_A$$

which can be rewritten as

$$(z_{CA}m_p)\dot{u} + (-x_{CA}m_p)\dot{w}$$

$$+(I_{yys} + Z_{CA}b_1 - x_{CA}c_1)\dot{q}_s$$

$$+(z_{CA}b_2 - x_{CA}c_2)\ddot{\phi} \qquad \text{III.41}$$

$$+(z_{CA}b_A - x_{CA}c_A)\ddot{\psi} =$$

$$M_T + M_A - z_{CA}b_3 + x_{CA}c_3$$

Combination of equations (III.34, III.35) and (III.17) results in

$$I_{yyp}\dot{q}_p - m_p\ell\cos\psi\dot{u} - b_1\ell\cos\psi\dot{q}_s$$
$$- b_2\ell\cos\psi\ddot{\phi} - b_4\ell\cos\psi\ddot{\psi} - b_3\ell\cos\psi$$
$$+ m_p\ell\sin\psi\dot{w} + c_1\ell\sin\psi\dot{q}_s$$
$$+ c_2\ell\sin\psi\ddot{\phi} + c_4\ell\sin\psi\ddot{\psi} + c_3\ell\sin\psi$$
$$= - M_B \qquad \text{(III.42)}$$

Finally, the quantity q_p can be related to q_s by

$$\begin{aligned} q_p &= q_s + \dot{\phi} + (\dot{\psi} - \dot{\phi}) \\ q_p &= q_s + \dot{\psi} \\ \dot{q}_p &= \dot{q}_s + \ddot{\psi} \end{aligned} \tag{III.43}$$

Combination of the last of equations (III.43) with (III.42) and rearranging terms results in

$$\begin{aligned} &(-m_p\, \ell\cos\psi)\dot{u} + (m_p\, \ell\sin\psi)\dot{w} \\ &\quad + (I_{yyp} - b_1\, \ell\cos\psi + c_1\, \ell\sin\psi)\dot{q}_s \\ &\quad + (-b_2\, \ell\cos\psi + c_2\, \ell\sin\psi)\ddot{\phi} \\ &\quad + (I_{yyp} - b_4\, \ell\cos\psi + c_4\, \ell\sin\psi)\ddot{\psi} \\ &= -M_B + b_3\, \ell\cos\psi - c_3\, \ell\sin\psi \end{aligned} \tag{III.44}$$

Equations (III.38), (III.39), (III.41), and (III.44) are four equations of the form

$$B_{i1}\dot{u} + B_{i2}\dot{w} + B_{i3}\,\dot{q}_s + B_{i4}\ddot{\phi} + B_{i5}\ddot{\psi} = D_i \quad (i=1,4) \tag{III.45}$$

This is a system of four equations with five unknowns.

Equation (III.13) can be used, along with (III.34) and (III.35) to obtain the needed additional relation. Equation (III.13) can be rewritten as shown below when A_z and A_x are eliminated.

$$\begin{aligned} &m_p d\cos\phi\,\dot{w} + c_1 d\cos\phi\dot{q}_s + c_2 d\cos\phi\ddot{\phi} + c_4 d\cos\phi\ddot{\psi} + c_3 d\cos\phi \\ &+ m_p d\sin\phi\,\dot{u} + b_1 d\sin\phi\dot{q}_s + b_2 d\sin\phi\ddot{\phi} + b_4 d\sin\phi\ddot{\psi} + b_3 d\sin\phi \\ &+ M_B - M_A = 0 \end{aligned}$$

which can be rewritten as

$$
\begin{aligned}
&(m_p d \sin\phi)\dot{u} + (m_p d \cos\phi)\dot{w} \\
&+ (b_1 d \sin\phi + c_1 d \cos\phi)\dot{q}_s \\
&+ (b_2 d \sin\phi + c_2 d \cos\phi)\ddot{\phi} \\
&+ (b_4 d \sin\phi + c_4 d \cos\phi)\ddot{\psi} \\
&= M_A - M_B - b_3 d \sin\phi - c_3 d \cos\phi
\end{aligned}
\tag{III.46}
$$

Equation (III.45) forms the fifth equation needed. Now if we let

$$\ddot{\phi} = \dot{\omega}_\phi$$
$$\ddot{\psi} = \dot{\omega}_\psi$$

and add the two differential equations

$$\dot{\phi} = \omega_\phi$$
$$\dot{\psi} = \omega_\psi$$

we will have seven first-order ordinary differential equations in seven unknowns.

The only step left is to specify the form of M_B. M_B must depend on the relative angular displacement of the payload with respect to the arm (measured from its initial relative angular displacement, and on the angular rate of the payload with respect to the arm. The geometry for this is shown in Figure III.4.

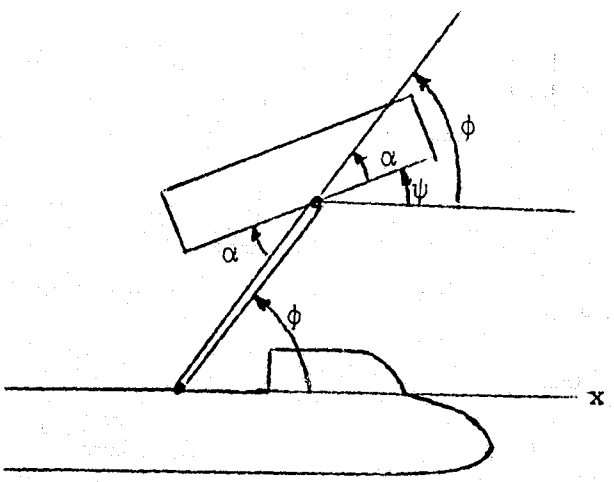

Figure III.4: Payload Angle Geometry

The required angle is α where

$$\alpha = \phi - \psi$$

Also,

$$\alpha_o = \phi_o - \psi_o$$

and

$$\dot{\alpha} = \dot{\phi} - \dot{\psi}$$

The torque, M_B, on the arm, is negative when $\alpha > \alpha_o$ and $\dot{\alpha} > 0$. Thus,

$$M_B = -K_B\ (\alpha - \alpha_o)\ -C_B\dot{\alpha}$$

or

$$M_B = -K_B\ (\phi - \psi - \phi_o + \psi_o)\ -C_B(\dot{\phi} - \dot{\psi}) \qquad \text{(III.47)}$$

The resultant elements of the b and D matrices are:

$B_{11} = (m_s + m_p)$

$B_{12} = 0$

$B_{13} = b_1$

$B_{14} = b_2$

$B_{15} = b_4$

$D_1 = T_x - m_s q_s w - b_3$

$B_{21} = 0$

$B_{22} = (m_s + m_p)$

$B_{23} = C_1$

$B_{24} = C_2$

$B_{25} = C_4$

$D_2 = T_z + m_s q_s u - c_3$

$B_{41} = -m_p \ell\cos\psi$

$B_{42} = m_p \ell\sin\psi$

$B_{43} = I_{yyp} - b_1 \ell\cos\psi + c_1 \ell\sin\psi$

$B_{44} = -b_2 \ell\cos\psi + c_2 \ell\sin\psi$

$B_{45} = I_{yyp} - b_4 \ell\cos\psi + c_4 \ell\sin\psi$

$D_4 = -M_B + b_3 \ell\cos\psi - c_3 \ell\sin\psi$

$B_{51} = m_p d\ \sin\phi$

$B_{52} = m_p d\ \cos\phi$

$B_{53} = b_1 d\ \sin\phi + c_1 d\ \cos\phi$

$B_{54} = b_2 d\ \sin\phi + c_2 d\ \cos\phi$

$B_{55} = b_4 d\ \sin\phi + c_4 d\ \cos\phi$

$D_5 = M_A - M_B - b_3 d\ \sin\phi - c_3 d\ \cos\phi$

$$B_{31} = z_{CA} m_p$$

$$B_{32} = (-x_{CA} m_p)$$

$$B_{33} = I_{yys} + z_{CA} b_1 - x_{CA} c_1$$

$$B_{34} = z_{CA} b_2 - x_{CA} c_2$$

$$B_{35} = z_{CA} b_4 - x_{CA} c_4$$

$$D_3 = M_T + M_A - z_{CA} b_3 + x_{CA} c_3$$

The solution procedure is the same as that outlined in Section II.

IV. NUMERICAL RESULTS

The one joint model developed in Section II and the two joint model developed in Section III have been compared for a series of thruster firing modes. The goal of this comparison was to determine the similarities and differences in the dynamics as predicted by the two models. An analysis made with the programs written to check the algebraic signs and the initial magnitudes (see Appendix A) indicated that for the loaded RMS extended vertically above the shuttle, Thruster 9 (the center RCS thruster firing upward on the shuttle nose) produced the largest forces and bending moments at the shoulder joint. All thrusters were checked in this determination.

Three comparison cases are presented here as an example of the data obtainable from the programs. The three cases assume that Thruster 9 is fired for 0.1 seconds and investigates the system oscillation during the subsequent 100 seconds. The parameters for each of the three cases are listed in Table 1.

The numerical results were obtained by numerically integrating equations (II.40) and (II.41) for the single joint model and equations (III.45) and (III.46) for the two joint model using the parameters listed in Table 1. The equations were integrated with a 4th-order Runge-Kutta integrator. The simulation assumes that the RMS is manipulating a cylindrical payload with a mass of slugs The numerical results obtained in this study are shown in Figures IV.1 through IV.6. Two separate cases were considered with the two-joint model. The cases differed in the length of the wrist joint. In Case II, the wrist joint was zero while in Case III the wrist joint was 7.5 ft.

Table 1. PARAMETERS FOR NUMERICAL SIMULATION

Program	Case 1 Single Joint	Case 2 Two Joint	Case 3 Two Joint
m_p	2018.5 slugs	Same as Case 1	Same as Case 1
m_s	4689.4 slugs	"	"
d	50 ft	"	"
$\dot{d}$	0	"	"
$\ddot{d}$	0	"	"
x_{CA}	36.33 ft	"	"
z_{CA}	-6.083 ft	"	"
C_A	1.22×10^5 lb.ft.sec/rad	"	"
K_A	1.0×10^4 lb.ft/radian	"	"
I_{YYS}	5699753. slug.ft^2	"	"
I_{YYP}	625805. slug.ft^2	"	"
T_x	0.0 lbs	"	"
T_z	870.0 lbs	"	"
u_o	0	"	"
w_o	0	"	"
q_{so}	0	"	"
$\omega_o = \omega_{\phi o}$	0	"	"
ϕ_o	90°	"	"
ℓ	---	0	7.5 ft
$\omega_{\psi o}$	---	0	0
ψ_o	---	0	0
C_B	---	1.22×10^5 lb.ft.sec/rad	Same as Case 2
K_B	---	1.0×10^4 lb.ft/rad	Same as Case 2
PLOT SYMBOL	△	⊡	◈

The data for Case 1 do not contain the wrist joint rate, joint angle, or moment at the wrist because these variables did not appear in the single joint model. These variables do, however, appear in Cases 2 and 3 which were generated using the two joint model. The output variables (all plotted versus time) for the three cases are as listed below.

SH VX — This is the x component (in body axes) of the velocity of the center of mass of the shuttle in

SH VZ — This is the z component of the velocity of the shuttle center of mass in ft/s.

QS — This is the pitch rate of the shuttle in degrees per second.

PHIDOT — This is the angular rate of the shoulder joint in degrees per second.

PHI — This is the shoulder angle in degrees

ALPHA DOT — This is the wrist joint rate (rate of rotation of the payload relative to the arm) in degrees per second. This variable is not integrated but is created after integration by differencing angular rates

ALPHA — This is the wrist joint angle in degrees. This variable is the angle between the arm and the payload x axis.

ARMFX($\equiv A_X$) — This is the x component of the force in pounds at the shoulder exerted on the shuttle by the RMS (The x component of force exerted on the payload by the wrist is -AX for an RMS which is modeled as massless).

ARM FZ($\equiv A_Z$) This is the Z component of the force in pounds at the shoulder exerted on the shuttle by the RMS.

AM($\equiv M_A$) This is the shoulder moment exerted by the RMS on the shuttle in ft. pounds.

BM($\equiv M_B$) This is the wrist moment exerted on the RMS by the payload in ft. pounds.

Figures IV.1 through IV.6 give 100-second time histories of all output variables for the three cases described previously. Recall that case 1 does not output the variables $\dot{\alpha}$ (ALPHADOT), α (ALPHA), and BM.

FIGURE IV.1

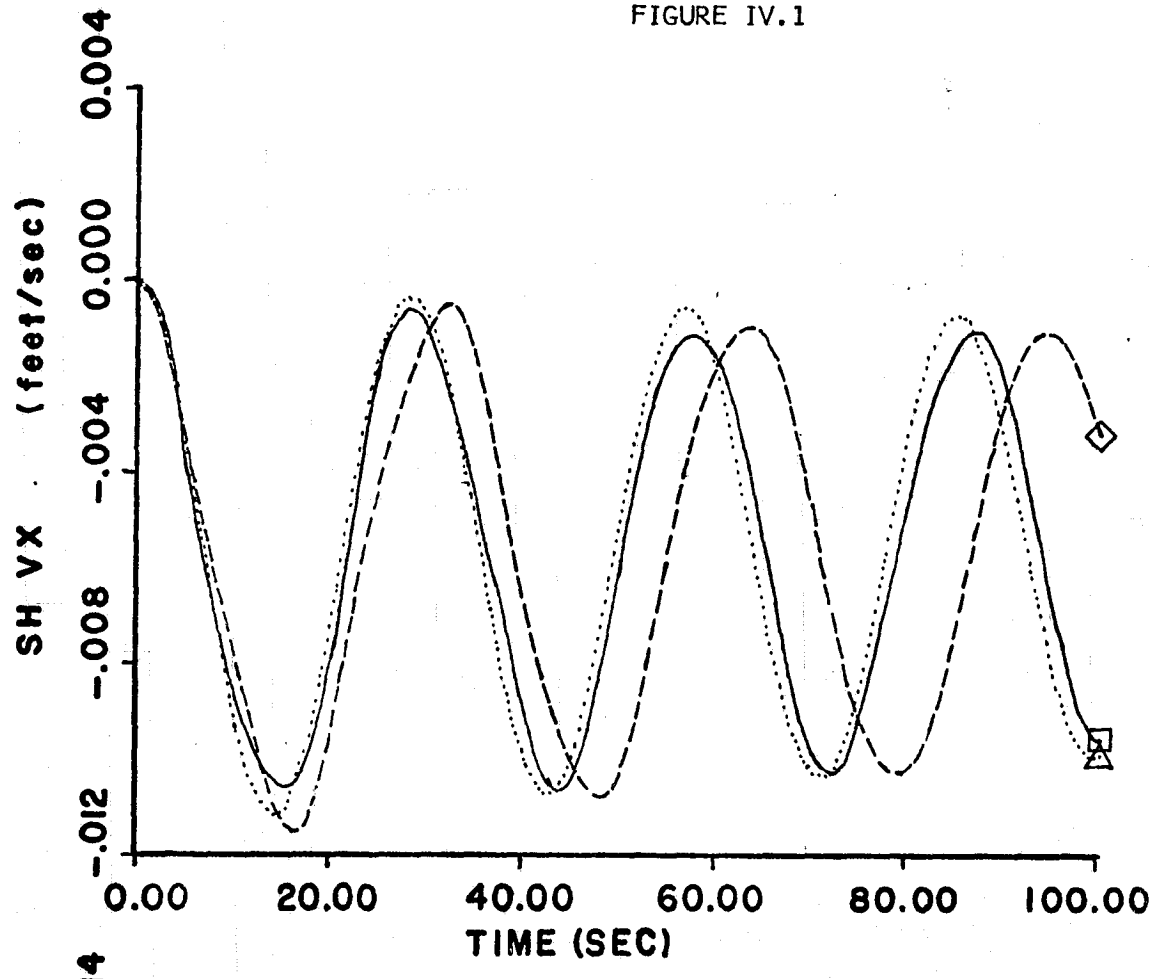
SH VX (feet/sec)
0.004
0.000
-.004
-.008
-.012
0.00
20.00
40.00
60.00
80.00
100.00
TIME (SEC)

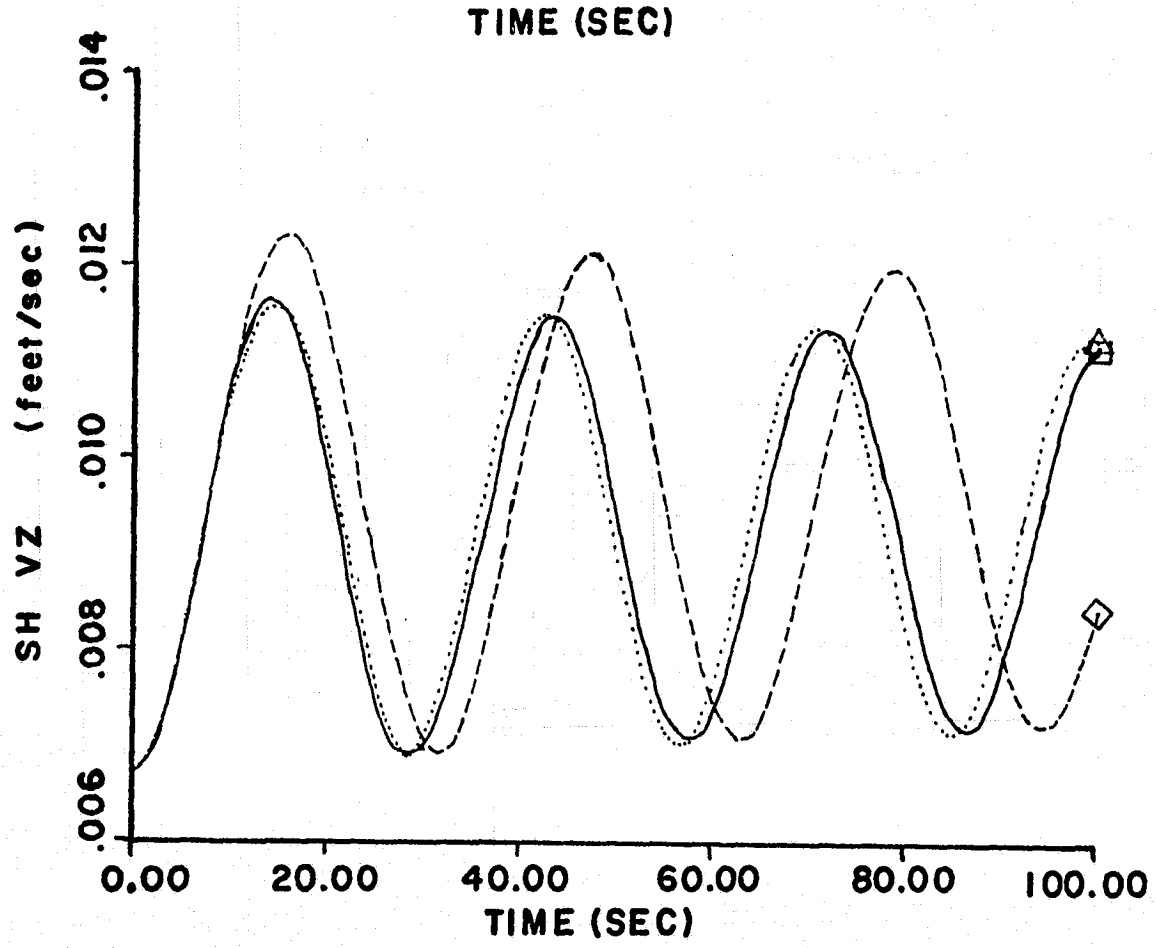
SH VZ (feet/sec)
.014
.012
.010
.008
.006
0.00
20.00
40.00
60.00
80.00
100.00
TIME (SEC)

FIGURE IV.2

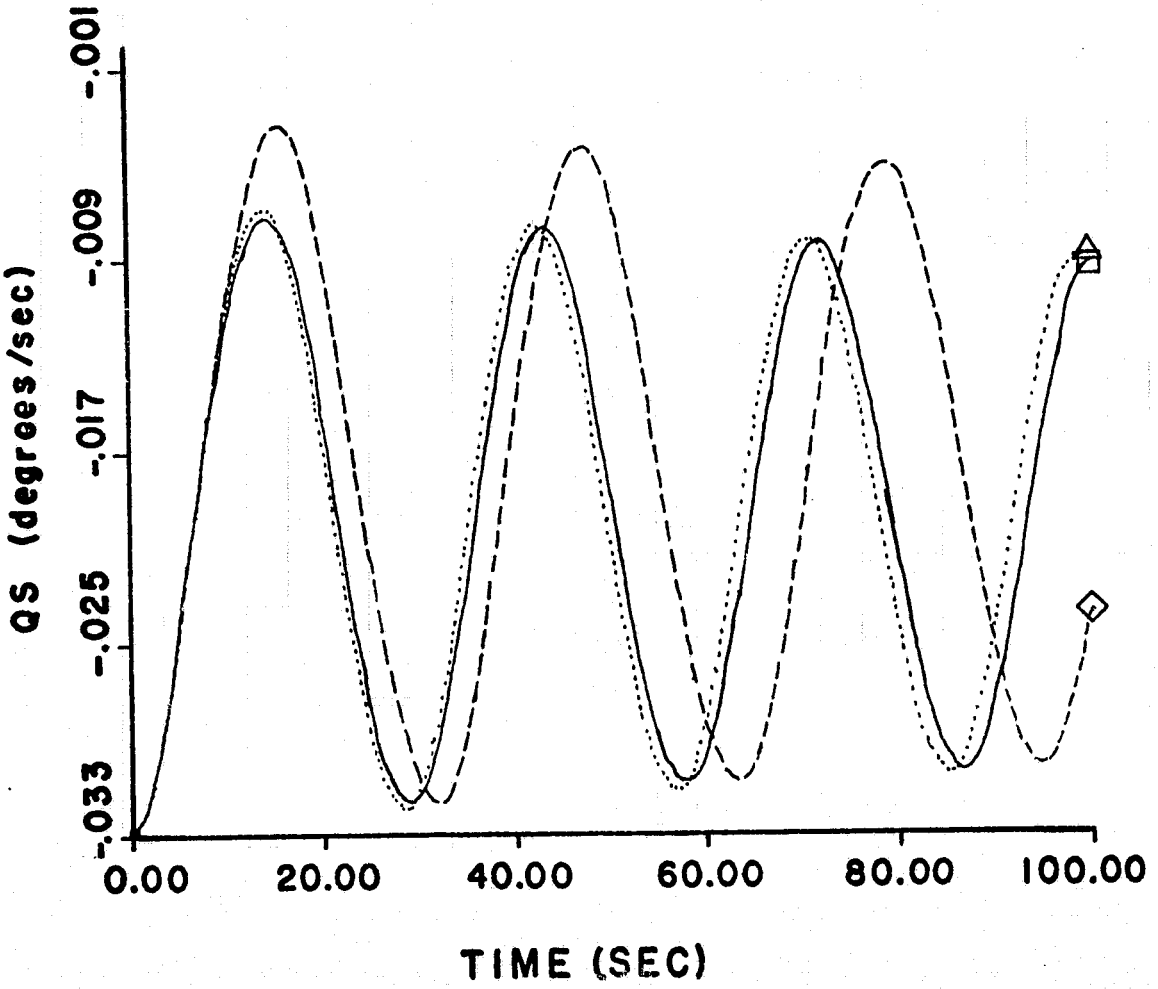
QS (degrees/sec)
-.001
-.009
-.017
-.025
-.033
0.00
20.00
40.00
60.00
80.00
100.00
TIME (SEC)

FIGURE IV.3

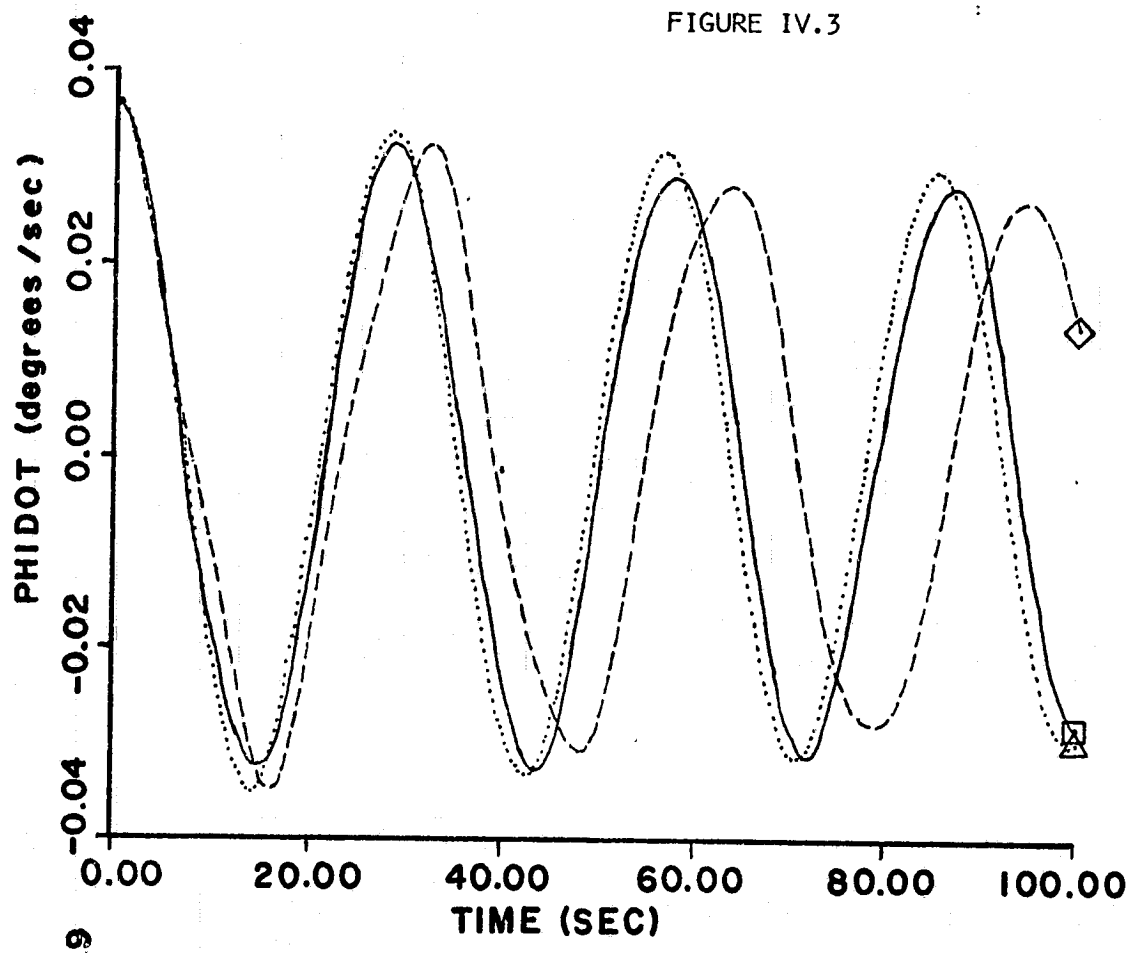
PHIDOT (degrees/sec)
0.04
0.02
0.00
-0.02
-0.04
0.00
20.00
40.00
60.00
80.00
100.00
TIME (SEC)

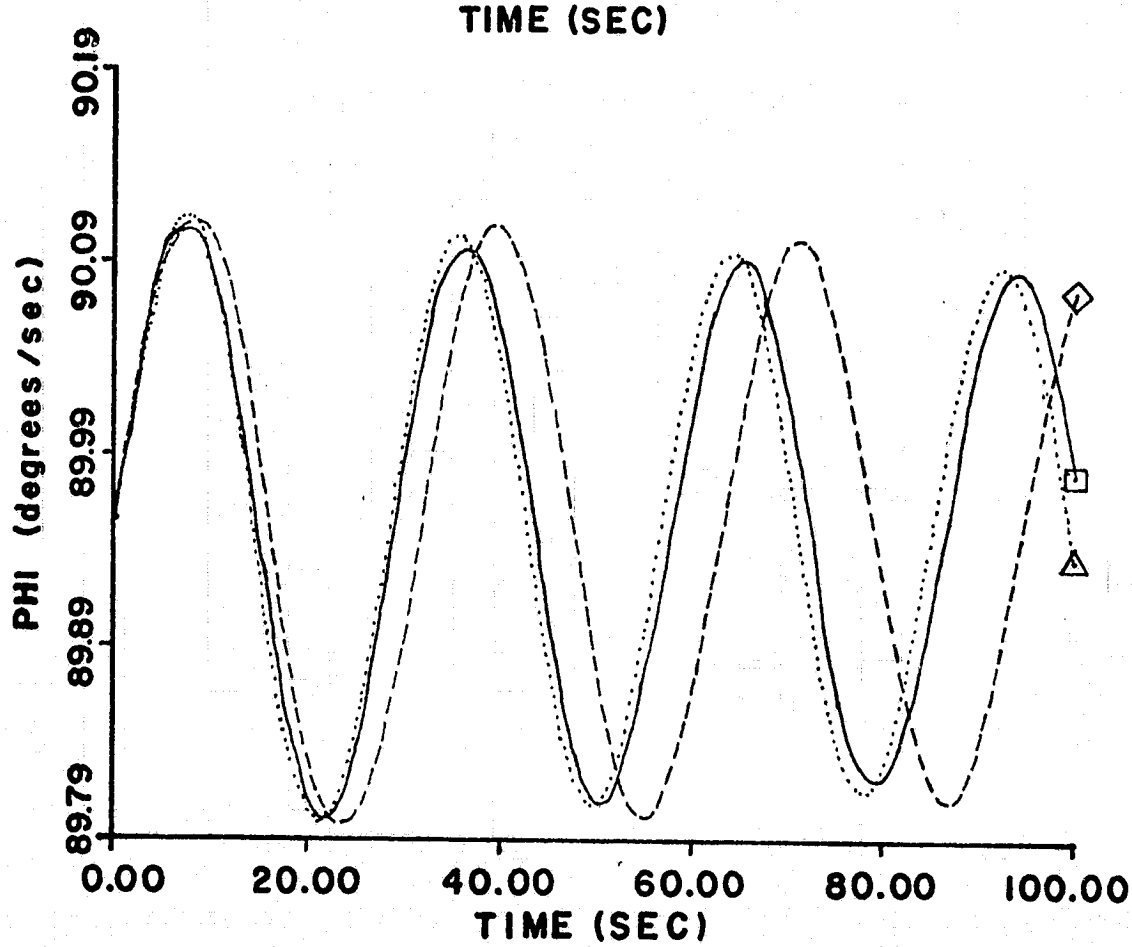
PHI (degrees/sec)
90.19
90.09
89.99
89.89
89.79
0.00
20.00
40.00
60.00
80.00
100.00
TIME (SEC)

FIGURE IV.4

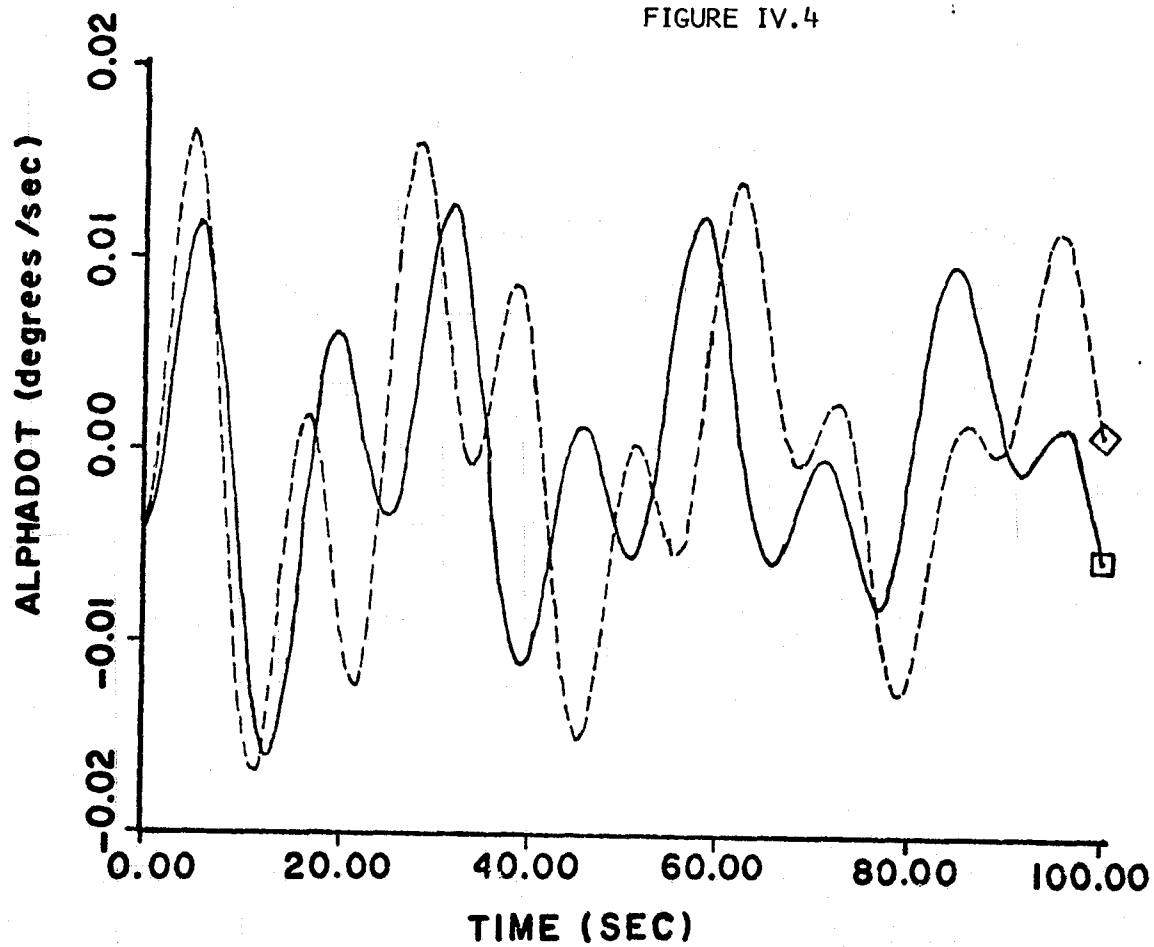
ALPHADOT (degrees/sec)
0.02
0.01
0.00
-0.01
-0.02
0.00
20.00
40.00
60.00
80.00
100.00
TIME (SEC)

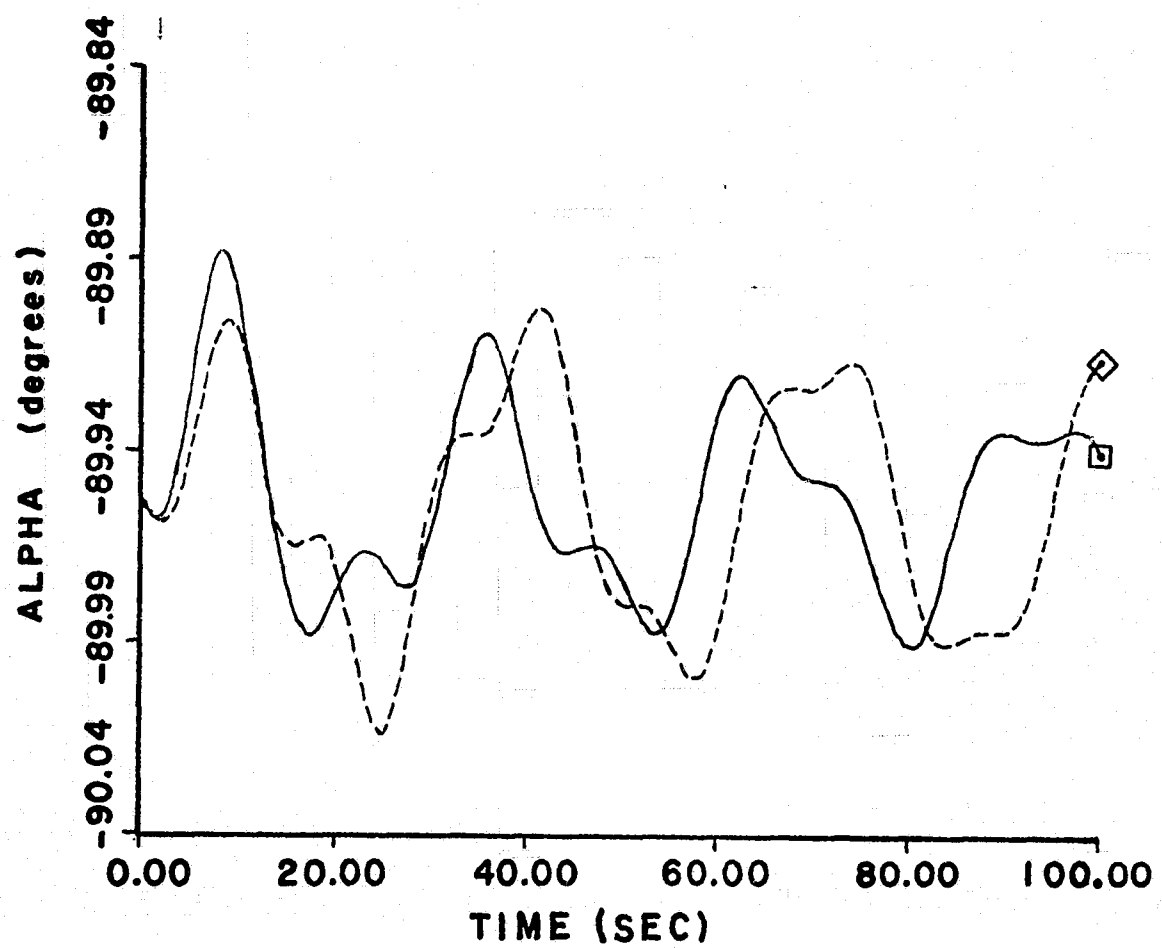
ALPHA (degrees)
-89.84
-89.89
-89.94
-89.99
-90.04
0.00
20.00
40.00
60.00
80.00
100.00
TIME (SEC)

FIGURE IV.5

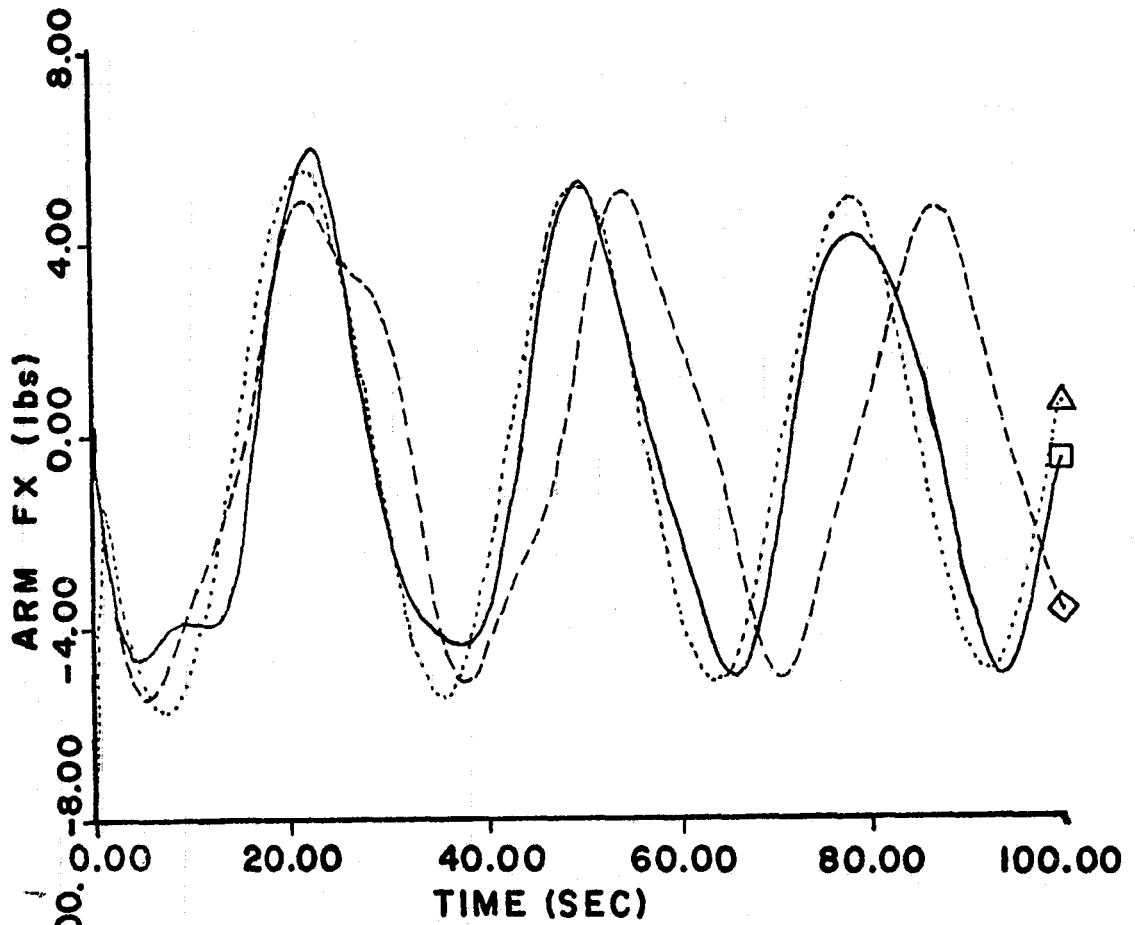
ARM FX (lbs)
8.00
4.00
0.00
-4.00
-8.00
0.00
20.00
40.00
60.00
80.00
100.00
TIME (SEC)

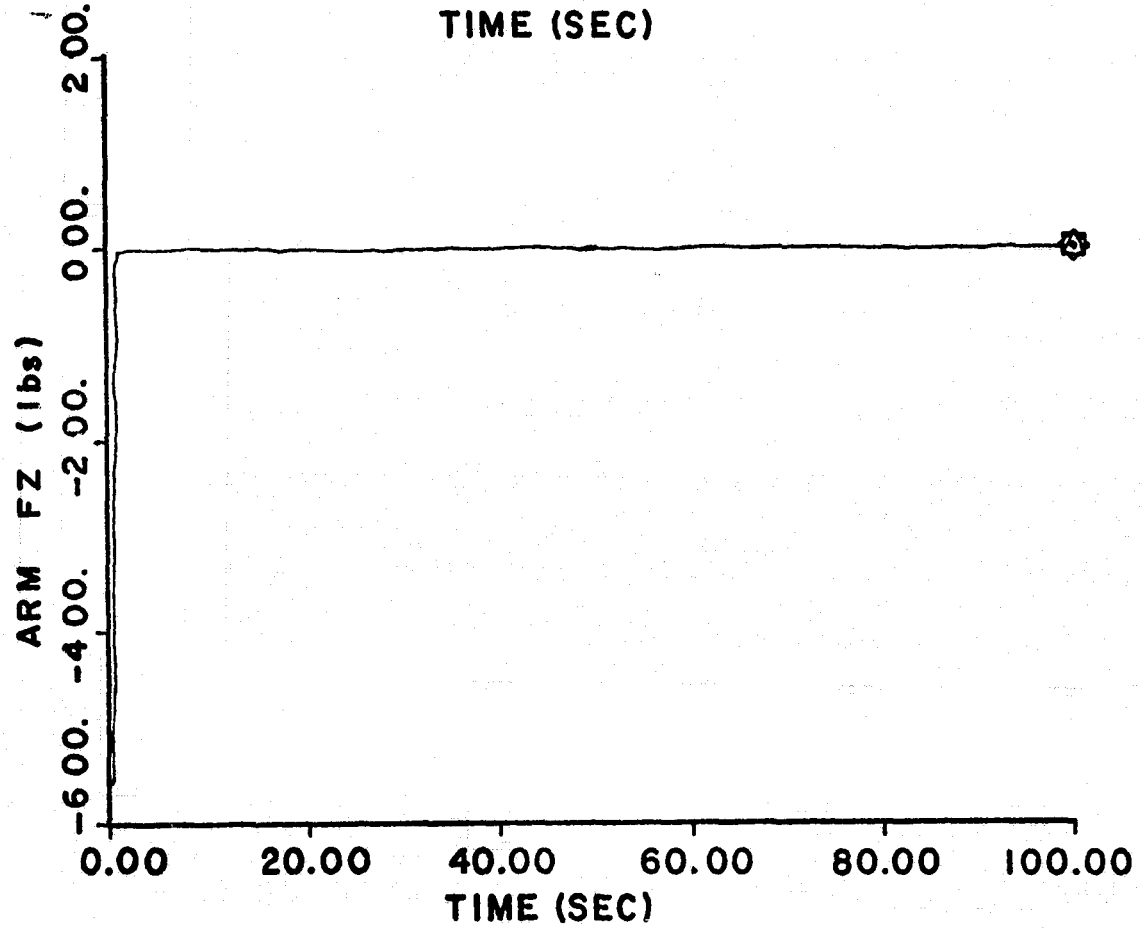
ARM FZ (lbs)
2.00.
0.00.
-2.00.
-4.00.
-6.00.
0.00
20.00
40.00
60.00
80.00
100.00
TIME (SEC)

FIGURE IV.6

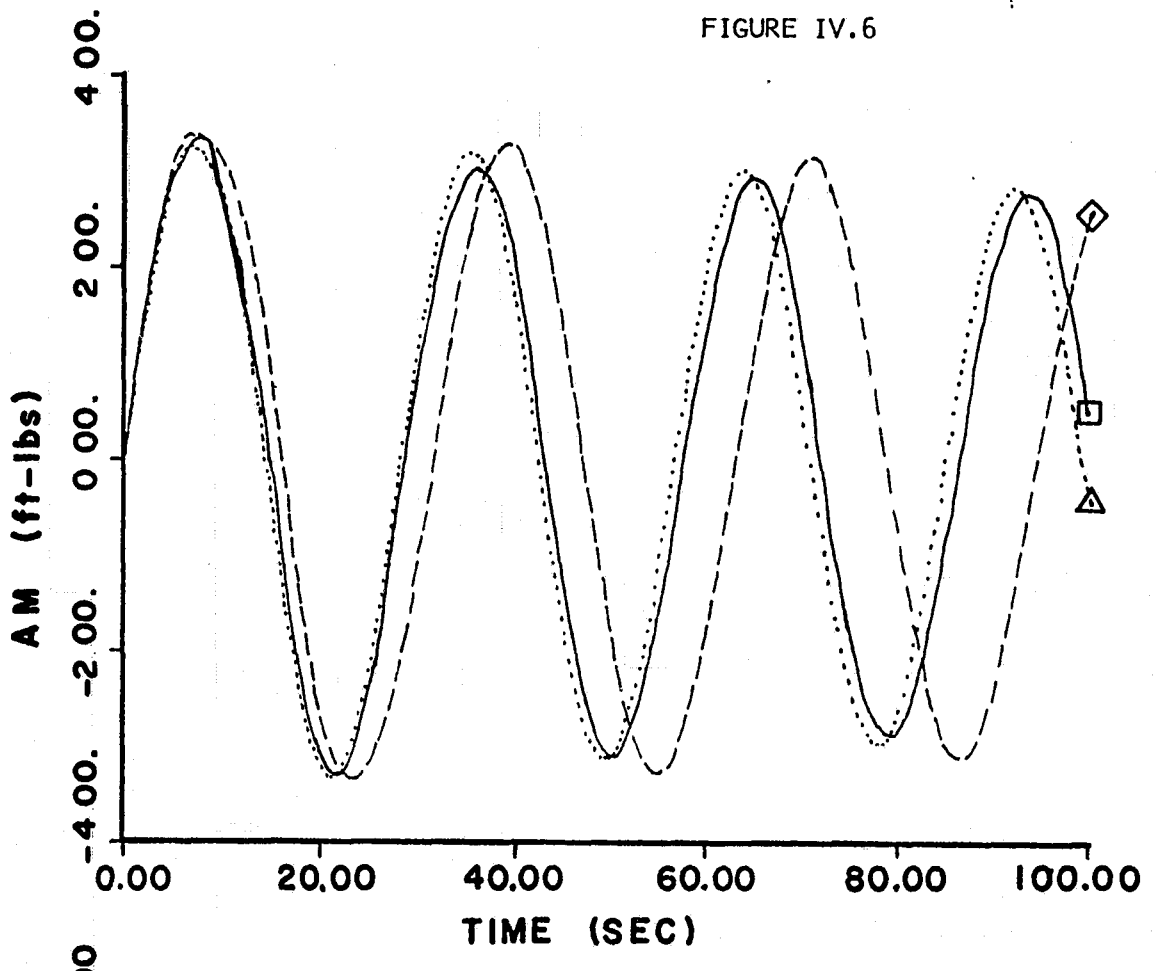
AM (ft-lbs)
4 00.
2 00.
0 00.
-2 00.
-4 00.
0.00
20.00
40.00
60.00
80.00
100.00
TIME (SEC)

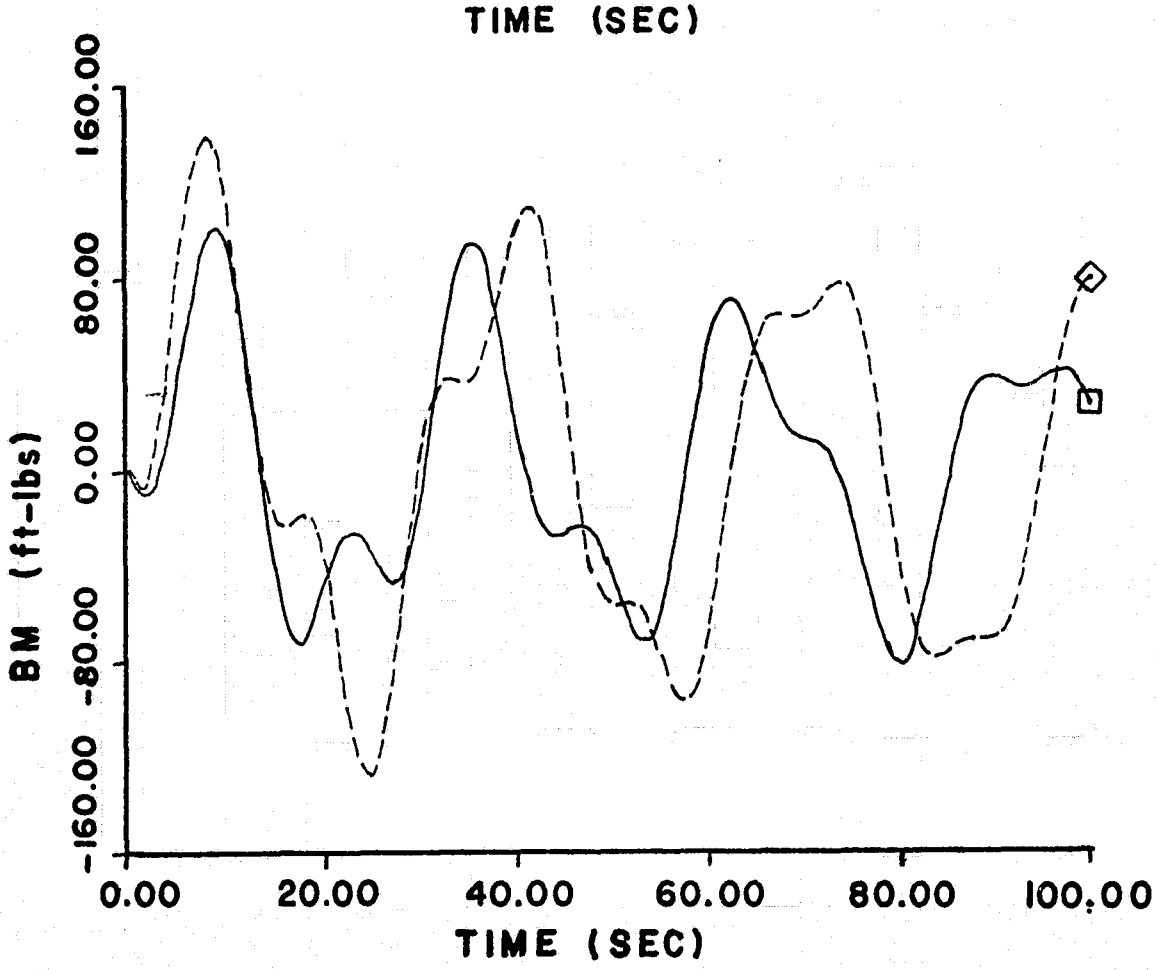
BM (ft-lbs)
160.00
80.00
0.00
-80.00
-160.00
0.00
20.00
40.00
60.00
80.00
100.00
TIME (SEC)

From the figures, it is apparent that the dynamic behavior of Case 1 (symbol△) matches that of Case 2 (symbol ⊡) quite well. Both amplitudes and periods of oscillations match very well. This match is significant because the case 1 curves (△) were produced with the single joint model while the Case 2 curves (⊡) were produced with the two joint model.

The similarities in dynamic behavior between Cases 1 and 2 can be attributed to the following factors:

1. The payload center of mass is the same distance from the shoulder (50 ft) in both cases.
2. The shoulder spring constant and damping constant are the same in both cases.
3. The excitation (Thruster 9) is the same in both cases.
4. The initial conditions are the same.

The differences between Cases 1 and 2 are as follows.

1. The wrist in Case 1 is rigid while there is a joint with a spring constant and dampoing at the wrist in Case 2.
2. No wrist joint torque is obtained in Case 1 (it could be obtained by a rigid-body analysis but would be far too large), while the torque is obtained in Case 2.

The results for Case 3 (symbol ◇) do not match the results of Cases 1 and 2 mainly because the payload, c.g., in this case is 7.5 feet away from the wrist joint (the more realistic case). In Cases 1 and 2 the payload is assumed to have its c.g. at the wrist joint (in all cases the payload has a non-zero moment of inertia about its center of mass).

The period of oscillation in Case 3 is longer than in Cases 1 and 2 (31 seconds as opposed to 27 seconds), largely because of the additional 7.5 feet between the payload center of mass and the shoulder joint (the pendulum is longer).

The magnitude of the oscillations in the x component of velocity of the shuttle's center of mass is about the same in all three cases whereas the z velocity component oscillation is slightly larger for Case 3. The amplitude of oscillation in shuttle pitch rate is also larger for Case 3 than for Cases 1 and 2.

The angle ϕ between the arm and the orbiter oscillates with about the same amplitude and rate variations in all three cases. However, integration over a longer time might reveal an energy exchange between the wrist and shoulder joints for the two joint cases (Cases 2 and 3). This should be looked into when the models are compared fully.

The angle α and its rate $\dot{\alpha}$ are defined only for Cases 2 and 3. After an initial jump of 0.05 radians during the thruster firing, the angle α oscillates over a range of about 0.1 degree in both cases. The differences in geometry between the two cases causes the curves for α and $\dot{\alpha}$ to differ between the cases.

The crucial values in the analysis are the magnitudes of forces and moments at the shouler (and wrist) joint(s). In all three cases, the force component in the z direction is the important force variable. Although the z component of force oscillates after the thruster is cut off in the same way that the x component oscillates, the oscillation cannot be seen on the plot because of the very high peak values of the z force which occur for all cases during the thruster firing (during the initial 0.1 seconds). The force peaks were in the range of 550 lbs to 600 lbs in all three cases. Due to the

geometry, this force is an axial force on the arm. This force acts at both joints (shoulder and wrist). For the values of system parameters chosen, the peak values of force at the joints occur during or at the end of the thruster firing after which the joint forces become very small.

The moments experienced at the shoulder and wrist joints peak 90° out of phase with the forces at the joints. The plots of AM (all three cases) and BM (two cases) show how the moments vary as a function of time. The maximum torques exerted at the shoulder are larger than those at the wrist for the values of system parameters chosen for the examples. This is because the mass (and moment of inertia) of the shuttle are larger than those of the payload.

Examination of the curve for the wrist moment (BM) indicates clearly the effect of payload rotation about the wrist joint. Case 3 with the payload c.g. offset from the joint gives higher values of wrist moment as would be expected. Also, the predominant period of oscillation is again longer for Case 3 than for Case 2.

V. SUMMARY, CONCLUSIONS AND RECOMMENDATIONS

Both single joint and two joint models have been developed for two-dimensional analysis of shuttle RMS joint loads. A limited comparison of the two models has been made which indicates the following.

1. In many situations, either the single joint model or the two joint model can be used to predict the approximate maximum magnitudes of shoulder joint loads (forces and moments).

2. The single joint model can be used to predict maximum wrist joint forces, but the two joint model must be used if information concerning the wrist joint moment is desired.

3. Both models give information on shuttle oscillations induced by the RMS/payload combination. The time histories of the oscillations at each joint are also available.

Both the one joint and two joint models are limited. The major limitations are as follows.

1. Both models are two-dimensional while the RMS/shuttle/payload system is a three-dimensional dynamical system.
2. The number of joints in the models is one or two while the number of joints on the actual RMS is actually six.

Although the two limitations listed above are major, the models developed should be quite useful because of the joint sequence on the RMS (three of the joints are collinear and occur in sequence - one at the shoulder, one at the elbow, and one at the wrist).

The procedure by which the models were developed is readily extendable to a three joint (elbow joint added) planar model. Such a model is the next logical step in building up to a simplified dynamic model of the three-dimensional shuttle/RMS/payload system which might be usable in a simulator (a full-blown dynamic model will have difficulties operating in real time, and real time is a must for training simulators).

It is recommended that the following items be studied further.

1. The three joint planar model should be developed.
2. A two joint, three-dimensional model should be developed (shoulder yaw and shoulder pitch).
3. A four joint, three-dimensional model should be developed as an extension of the model of (2) above, and then a three-dimensional six joint model should be developed. The philosophy of each model should be to keep it as simple as possible while performing the required tasks.
4. The models completed should be compared, and versions selected for use as needed in:

    (a) training simulators,
    (b) mission planning and sequencing programs, and
    (c) engineering simulators.

PRECEDING PAGE BLANK NOT FILMED

PRECEDING PAGE BLANK NOT F.

APPENDIX A

ANALYSIS TO CHECK SIGNS OF A_x, A_z, etc. at t = 0

SINGLE JOINT MODEL

All rates will initially be zero, and quantities will be determined only at the instant when the thruster is turned on. Equations (II.1) through (II.3) are

$$T_x + A_x = m_s(\dot{u} + q_s w) \tag{II.1}$$

$$T_z + A_z = m_s(\dot{w} - q_s u) \tag{II.2}$$

$$M_A + z_{CA}A_x - x_{CA}A_z + M_T = I_{yys}\dot{q}_s \tag{II.3}$$

At t = 0, $q_s = w = u = 0$. Also, $\phi = \phi_o$, and $\dot{\phi} = 0$. Thus, from equation (II.34), i.e., assume also that $\ddot{d} = \dot{d} = 0$.

$$M_A = K(\phi - \phi_o) + C\dot{\phi} \tag{II.34}$$

it can be seen that $M_A = 0$ (at t = 0). Thus, equations (II.1) through (II.3) become

$$T_x + A_x = m_s\dot{u} \tag{A.1}$$

$$T_z + A_z = m_s\dot{w} \tag{A.2}$$

$$z_{CA}A_x - x_{CA}A_z + M_T = I_{yys}\dot{q}_s \tag{A.3}$$

From equations (II.28) and (II.32), we have

$$-A_x = m_p\dot{u} + b_1\dot{q}_s + b_2\ddot{\phi} + b_3 \tag{II.28}$$

$$-A_z = m_p\dot{w} + c_1\dot{q}_s + c_2\ddot{\phi} + c_3 \tag{II.32}$$

where, from equations (II.27) and (II.31) give b_1, b_2, b_3 and c_1, c_2, c_3, respectively. At t = 0, these values are

$$b_1 = m_p(z_{CA} - d \sin\phi)$$

$$b_2 = -m_p d \sin\phi$$

$$b_3 = 0$$

$$c_1 = (-x_{CA} - d \cos\phi)m_p$$

$$c_2 = -m_p(d \cos\phi)$$

$$c_3 = 0$$

Thus, (II.28) and (II.32) can be rewritten as

$$-A_x = m_p\dot{u} + b_1\dot{q}_s + b_2\ddot{\phi} \qquad (A.4)$$

$$-A_z = m_p\dot{w} + c_1\dot{q}_s + c_2\ddot{\phi} \qquad (A.5)$$

Equation (II.38) can be written at t = 0 as

$$(-m_p d \sin\phi)\dot{u} + (-m_p d \cos\phi)\dot{w} + (I_{yyp} - b_1 d \sin\phi - c_1 d \cos\phi)\dot{q}_s + (I_{yyp} - c_2 d \cos\phi - b_2 d \sin\phi)\ddot{\phi} = 0 \qquad (A.6)$$

Equations (A.1) through (A.6) form a system of six linear equations in six unknowns.

The equations, in matrix form, can be written as shown on the following page.

$$
\begin{bmatrix}
m_s & 0 & 0 & 0 & -1 & 0 \\
0 & m_s & 0 & 0 & 0 & -1 \\
0 & 0 & I_{yys} & 0 & -z_{CA} & x_{CA} \\
m_p & 0 & b_1 & b_2 & 1 & 0 \\
0 & m_p & c_1 & c_2 & 0 & 1 \\
-m_p d \sin\phi & -m_p d \cos\phi & \begin{matrix} I_{yyp} - \\ b_1 d \sin\phi \\ -c_1 d \cos\phi \end{matrix} & \begin{matrix} I_{yyp} - \\ c_2 d \cos\phi \\ -b_2 d \sin\phi \end{matrix} & 0 & 0
\end{bmatrix}
\begin{Bmatrix}
\dot{u} \\ \dot{w} \\ \dot{q}_s \\ \ddot{\phi} \\ A_x \\ A_z
\end{Bmatrix}
=
\begin{Bmatrix}
T_x \\ T_z \\ M_T \\ 0 \\ 0 \\ 0
\end{Bmatrix}
$$

TWO JOINT MODEL

Equations (III.1) through (III.3), with the assumptions $q_s = u = w = 0$, $M_A = 0$ gives (also $\dot{d} = \ddot{d} = 0$)($\dot{\phi} = \dot{\psi} = 0$, $\phi = \phi_o, \psi = \psi_o$)

$$m_s\dot{u} - A_x = T_x \tag{A.7}$$

$$m_s\dot{w} - A_z = T_z \tag{A.8}$$

$$I_{yys}\dot{q}_s + x_{CA}A_z - z_{CA}A_x = M_T \tag{A.9}$$

Equation (III.13) given $M_B = 0$ at $t = 0$, gives

$$A_x\, d\, \sin\phi + A_z\, d\, \cos\phi = 0 \tag{A.10}$$

Equation (III.17) can be written as

$$I_{yyp}\dot{q}_s + I_{yyp}\ddot{\psi} + A_x\, \ell\cos\psi - A_x\, \ell\sin\psi = 0 \tag{A.11}$$

Equations (III.34) and (III.35) can be written as

$$m_p\dot{u} + b_1\dot{q}_s + b_2\ddot{\phi} + b_4\ddot{\psi} + A_x = -\cancel{b_3}^{\,0} \tag{A.12}$$

$$m_p\dot{w} + c_1\dot{q}_s + c_2\ddot{\phi} + c_4\ddot{\psi} + A_z = -\cancel{c_3}^{\,0} \tag{A.13}$$

Where, from equations (III.32), (III.33), and the assumptions, we have

$$b_1 = m_p(z_{CA} - d\, \sin\phi - \ell\cos\psi)$$

$$b_2 = m_p(-d\, \sin\phi)$$

$$b_3 = 0$$

$$b_4 = m_p(-\ell\cos\psi)$$

$$c_1 = m_p(-x_{CA} - d\, \cos\phi + \ell\sin\psi)$$

$$c_2 = m_p(-d\, \cos\psi)$$

$$c_3 = 0$$

$$c_4 = m_p(\ell\sin\psi)$$

NOTE: b_1, b_2, b_4 and c_1, c_2, c_4 are formed as in TWØJNT.

The required matrix is given by writing equations (A.7) through (A.13) in matrix form, i.e.,

$$\begin{bmatrix} m_s & 0 & 0 & 0 & 0 & -1 & 0 \\ 0 & m_s & 0 & 0 & 0 & 0 & -1 \\ 0 & 0 & I_{yys} & 0 & 0 & -z_{CA} & +x_{CA} \\ 0 & 0 & 0 & 0 & 0 & d\sin\phi & d\cos\phi \\ 0 & 0 & I_{yyp} & 0 & I_{yyp} & \ell\cos\psi & -\ell\sin\psi \\ m_p & 0 & b_1 & b_2 & b_4 & 1 & 0 \\ 0 & m_p & c_1 & c_2 & c_A & 0 & 1 \end{bmatrix} \begin{Bmatrix} \dot{u} \\ \dot{w} \\ \dot{q}_s \\ \ddot{\phi} \\ \ddot{\psi} \\ A_x \\ A_z \end{Bmatrix} = \begin{Bmatrix} T_x \\ T_x \\ M_T \\ 0 \\ 0 \\ 0 \\ 0 \end{Bmatrix}$$